

Waves in Sea Ice

Kenneth M. Golden University of Utah



ICIAM 2019 Valencia

SEA ICE covers ~12% of Earth's ocean surface

- boundary between ocean and atmosphere
- mediates exchange of heat, gases, momentum
- global ocean circulation
- hosts rich ecosystem
- indicator of **climate change**



polar ice caps critical
to climate in reflecting
sunlight during summer

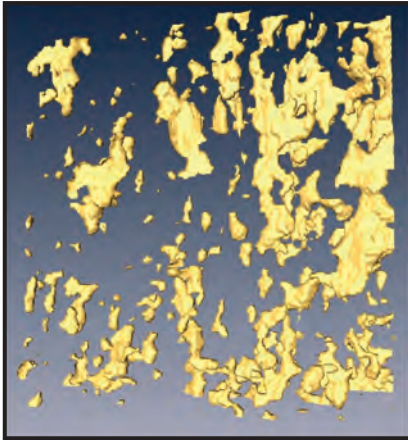
Sea Ice is a Multiscale Composite Material

sea ice microstructure

brine inclusions

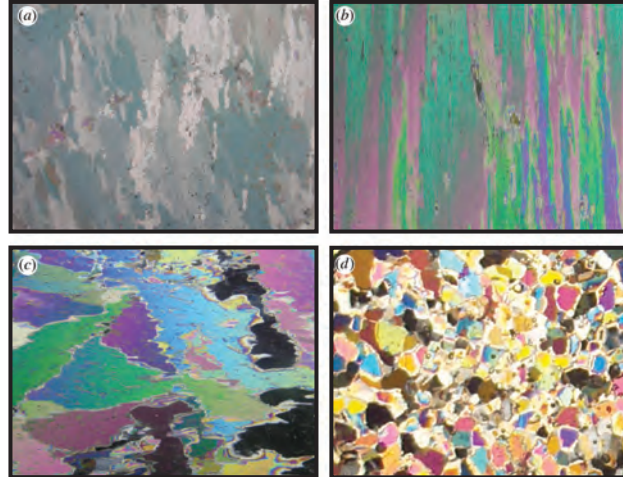


Weeks & Assur 1969



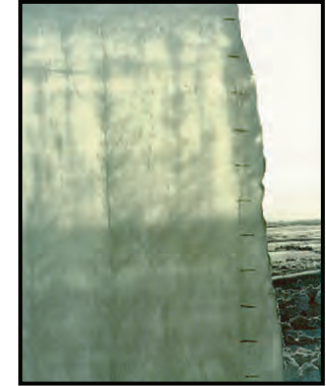
H. Eicken
Golden et al. GRL 2007

polycrystals

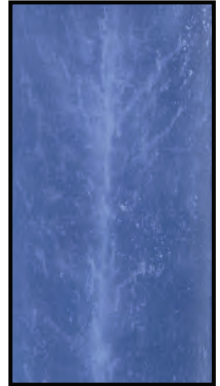


Gully et al. Proc. Roy. Soc. A 2015

brine channels



D. Cole



K. Golden

millimeters

centimeters

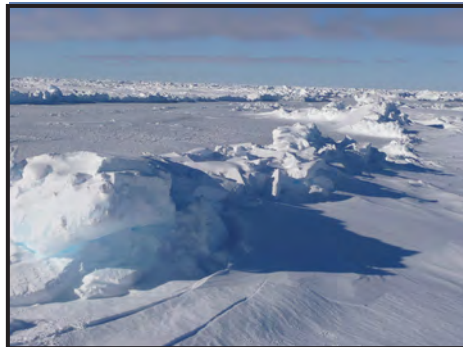
sea ice mesostructure

Arctic melt ponds



K. Frey

Antarctic pressure ridges



K. Golden

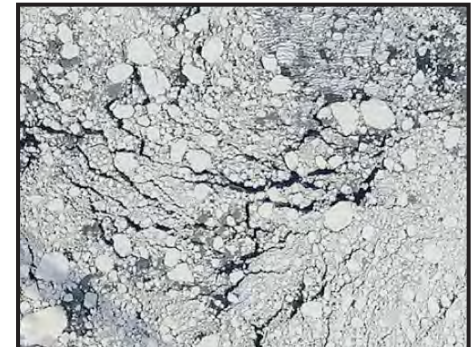
sea ice macrostructure

sea ice floes



J. Weller

sea ice pack



NASA

meters

kilometers

What is this talk about?

HOMOGENIZATION

Using methods of statistical physics and composite materials to LINK SCALES in the sea ice system ... rigorously compute effective behavior and improve climate models.

Tour wave phenomena in sea ice

1. Sea ice microphysics and fluid transport

homogenization and percolation theory

2. EM monitoring of sea ice, analytic continuation method

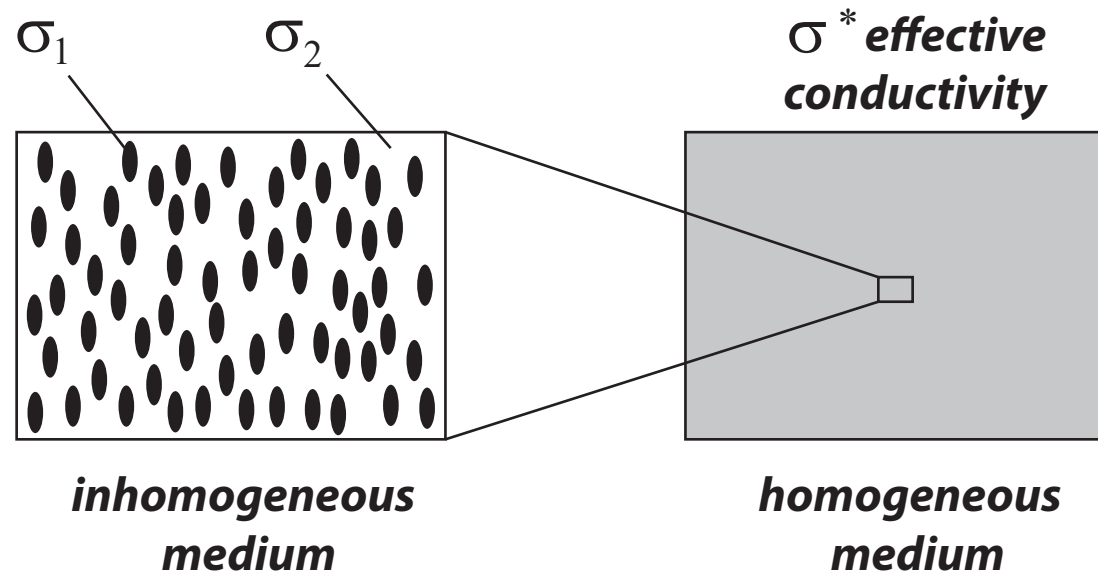
random matrix theory and Anderson transitions

3. Extension of ACM to polycrystals, waves in sea ice

Stieltjes integral representations, spectral measures

4. Light in sea ice, melt ponds

HOMOGENIZATION - Linking Scales in Composites



find the homogeneous medium which behaves macroscopically the same as the inhomogeneous medium

Maxwell 1873 : effective conductivity of a dilute suspension of spheres

Einstein 1906 : effective viscosity of a dilute suspension of rigid spheres in a fluid

*Wiener 1912 : arithmetic and harmonic mean **bounds** on effective conductivity*

*Hashin and Shtrikman 1962 : variational **bounds** on effective conductivity*

widespread use of composites in late 20th century due in large part to advances in mathematically predicting their effective properties

How do scales interact in the sea ice system?

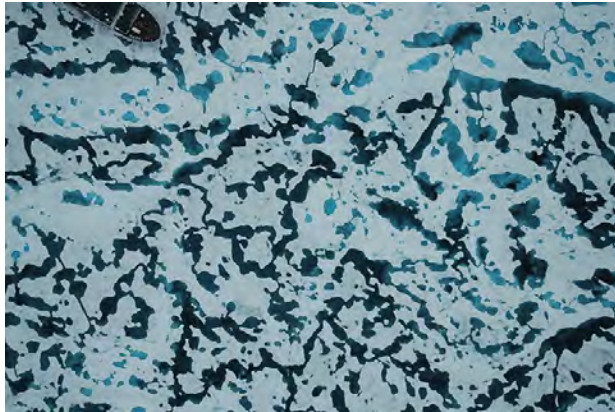


basin scale -
grid scale
albedo

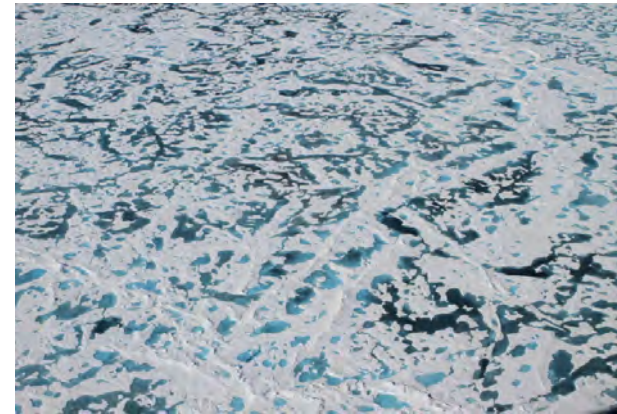
NASA

Linking Scales

km
scale
melt
ponds



km
scale
melt
ponds

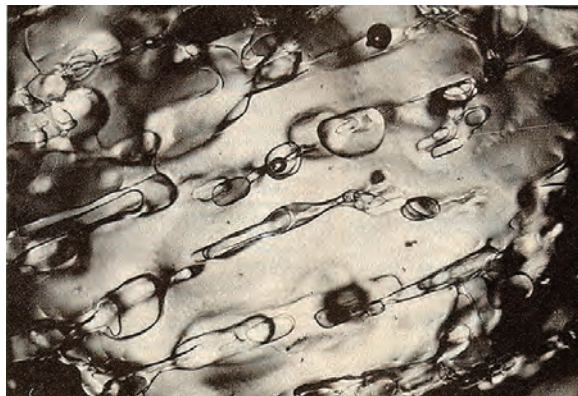


Perovich

Linking

Scales

mm
scale
brine
inclusions



meter
scale
snow
topography



sea ice microphysics

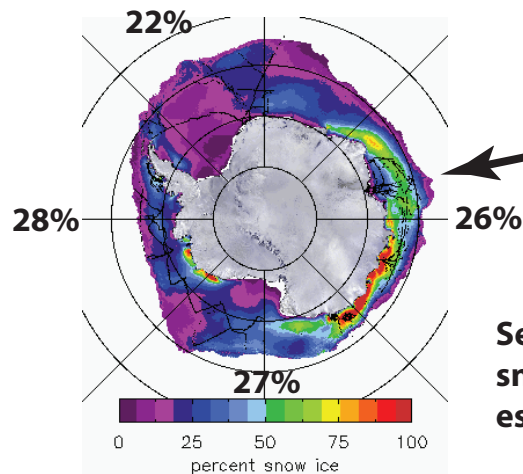
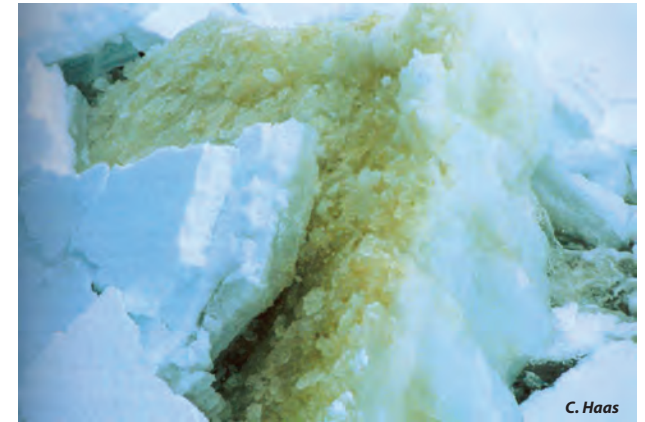
fluid transport

fluid flow through the porous microstructure of sea ice governs key processes in polar climate and ecosystems

evolution of Arctic melt ponds and sea ice albedo



nutrient flux for algal communities



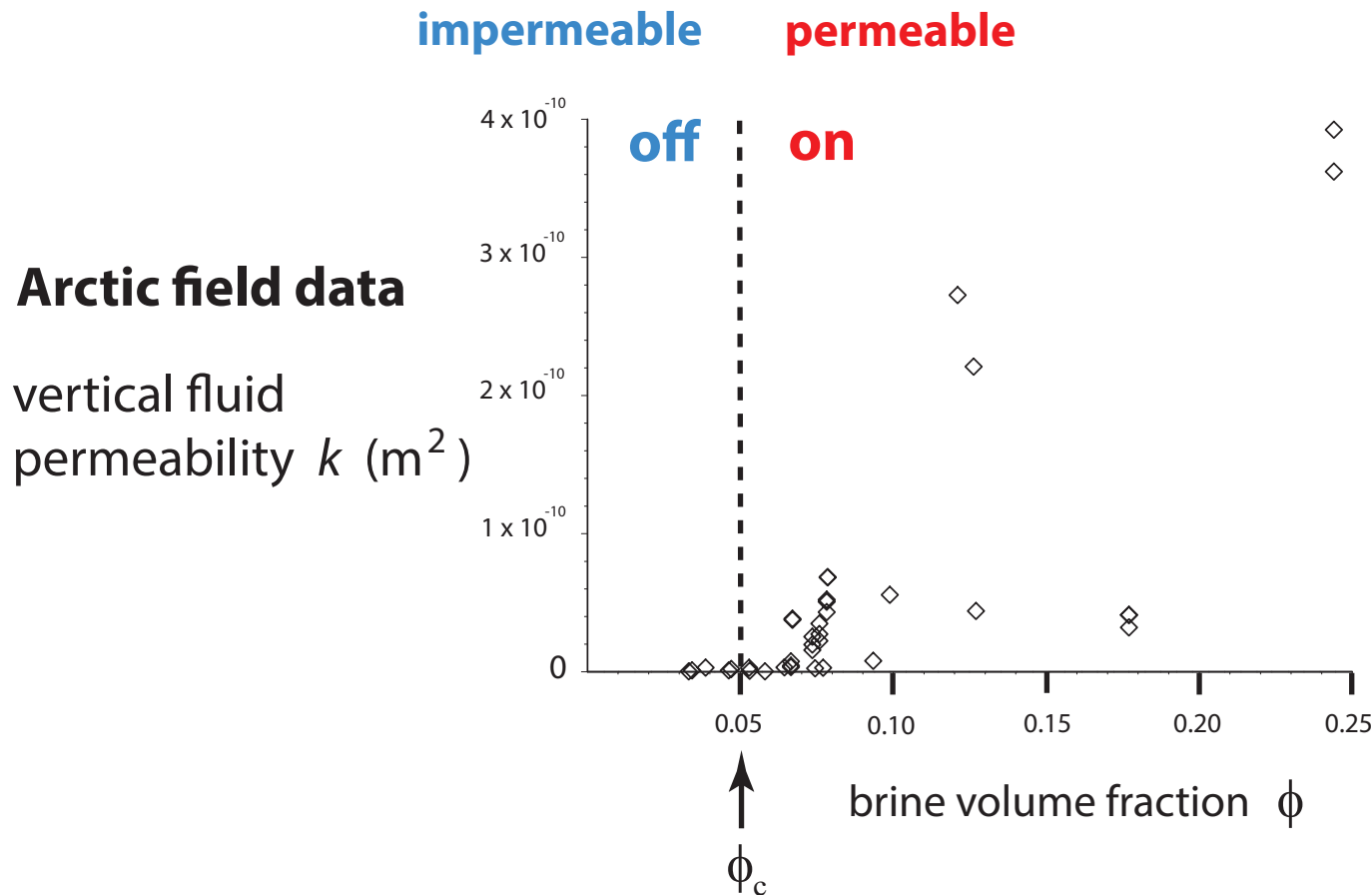
T. Maksym and T. Markus, 2008

*Antarctic surface flooding
and snow-ice formation*

September
snow-ice
estimates

- *evolution of salinity profiles*
- *ocean-ice-air exchanges of heat, CO₂*

Critical behavior of fluid transport in sea ice



***“on - off” switch
for fluid flow***

critical brine volume fraction $\phi_c \approx 5\% \longleftrightarrow T_c \approx -5^\circ \text{C}, S \approx 5 \text{ ppt}$

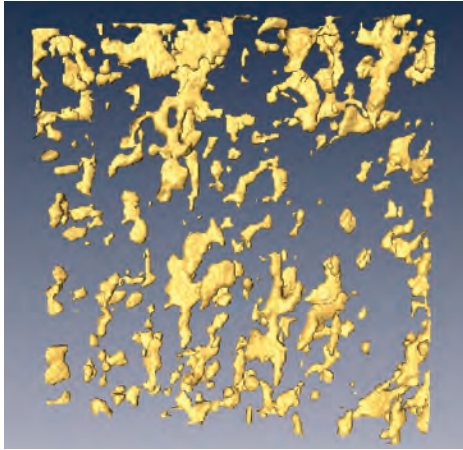
RULE OF FIVES

Golden, Ackley, Lytle Science 1998

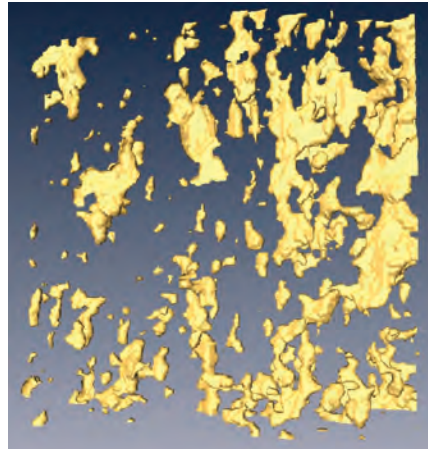
Golden, Eicken, Heaton, Miner, Pringle, Zhu GRL 2007

Pringle, Miner, Eicken, Golden J. Geophys. Res. 2009

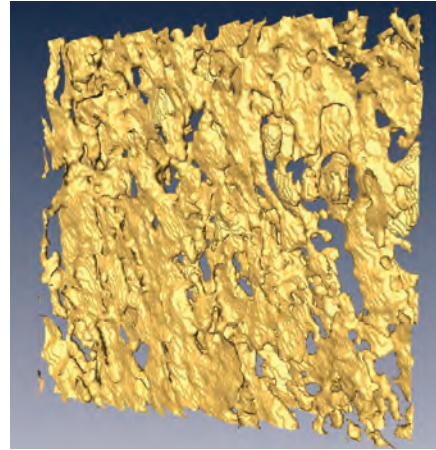
brine volume fraction and **connectivity** increase with temperature



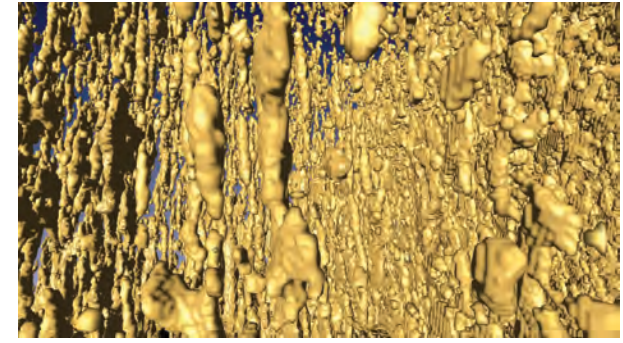
$T = -15\text{ }^{\circ}\text{C}$, $\phi = 0.033$



$T = -6\text{ }^{\circ}\text{C}$, $\phi = 0.075$



$T = -3\text{ }^{\circ}\text{C}$, $\phi = 0.143$



$T = -4\text{ }^{\circ}\text{C}$, $\phi = 0.113$

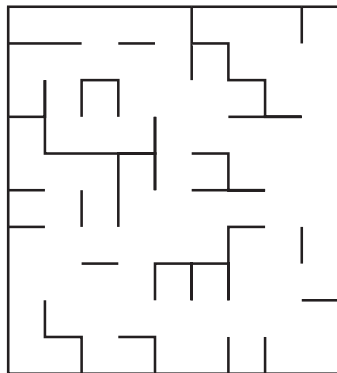
X-ray tomography for brine phase in sea ice

Golden, Eicken, *et al.*, *Geophysical Research Letters* 2007

PERCOLATION THRESHOLD $\phi_c \approx 5\%$

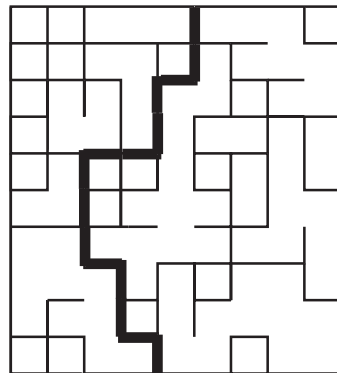
Golden, Ackley, Lytle, *Science* 1998

impermeable



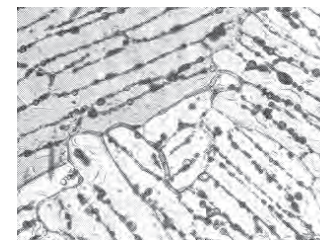
$p = 1/3$

permeable

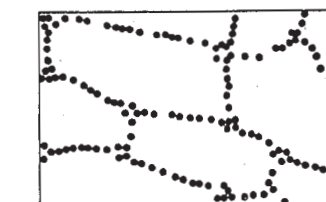
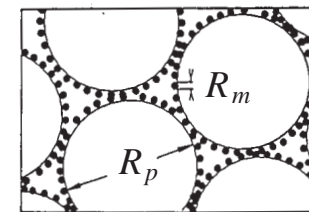


$p = 2/3$

lattice percolation



sea ice



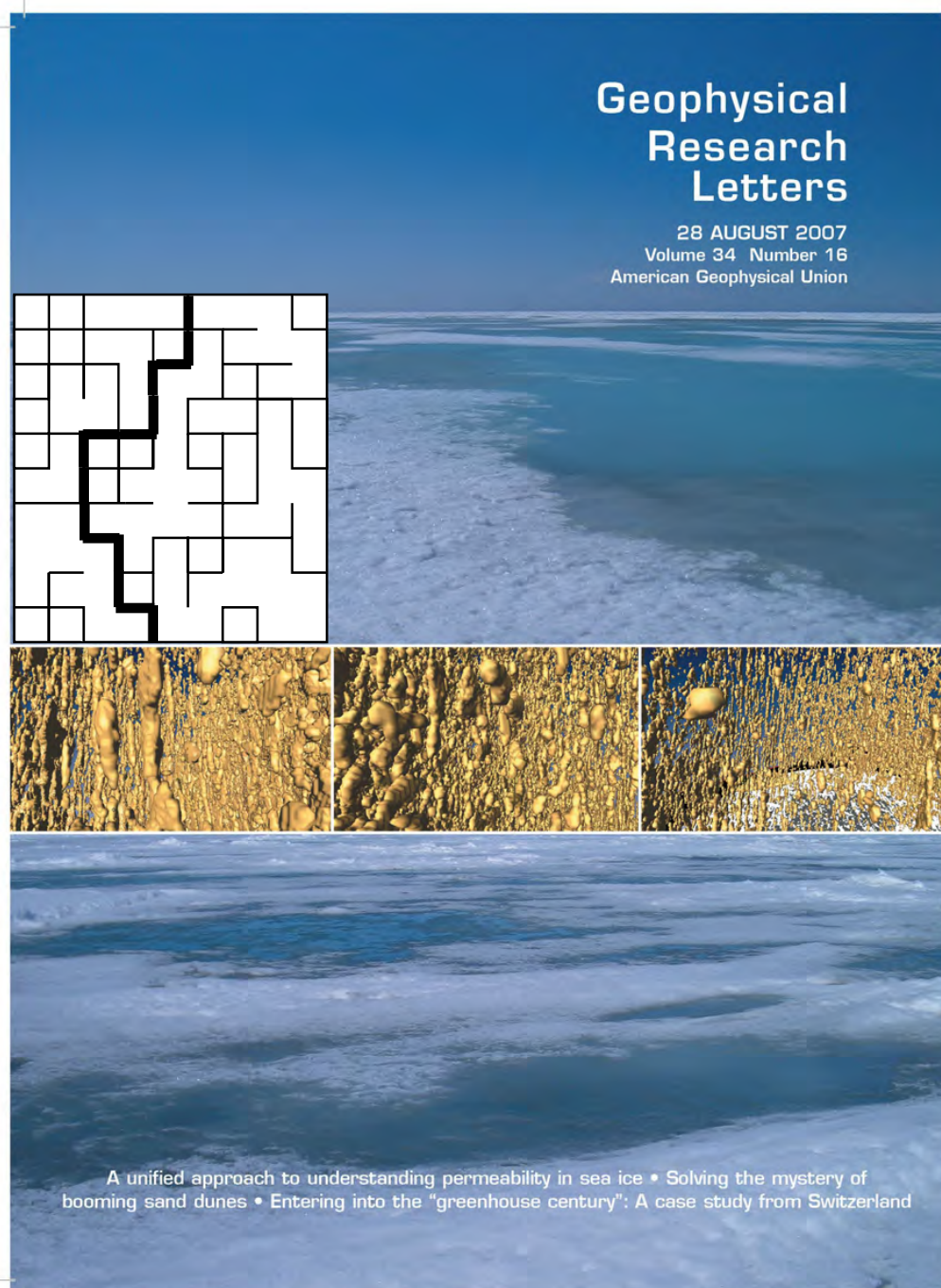
compressed powder

Kusy, Turner
Nature 1971

continuum percolation

Thermal evolution of permeability and microstructure in sea ice

Golden, Eicken, Heaton, Miner, Pringle, Zhu, Geophysical Research Letters 2007



micro-scale
controls
macro-scale
processes

percolation theory

$$k(\phi) = k_0 (\phi - 0.05)^2$$

critical
exponent
t

$$k_0 = 3 \times 10^{-8} \text{ m}^2$$

***hierarchical model
network model
rigorous bounds***

agree closely
with field data

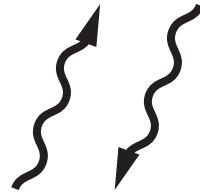
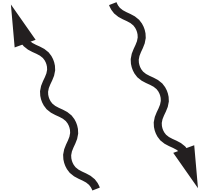
***X-ray tomography for
brine inclusions***

***unprecedented look
at thermal evolution
of brine phase and
its connectivity***

confirms rule of fives

***Pringle, Miner, Eicken, Golden
J. Geophys. Res. 2009***

Remote sensing of sea ice



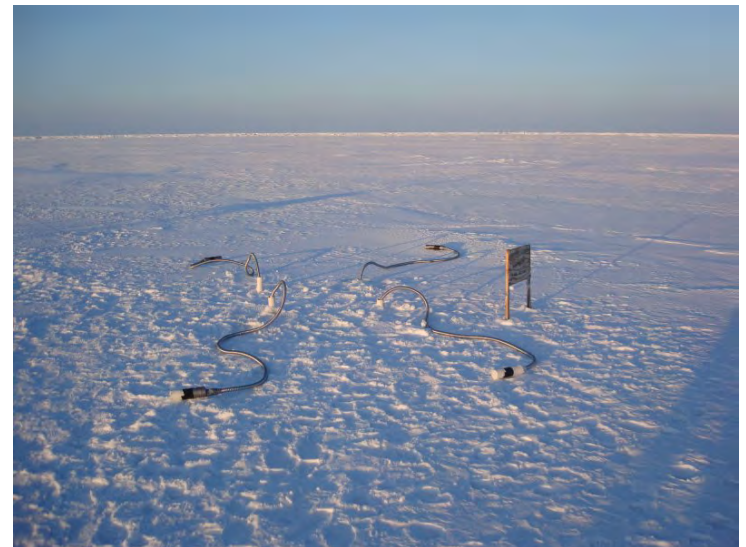
sea ice thickness
ice concentration

INVERSE PROBLEM

Recover sea ice
properties from
electromagnetic
(EM) data

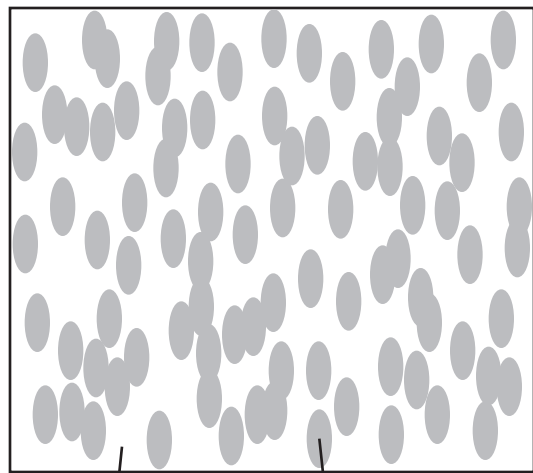
$$\epsilon^*$$

effective complex permittivity
(dielectric constant, conductivity)



brine volume fraction
brine inclusion connectivity

Effective complex permittivity of a two phase composite in the quasistatic (long wavelength) limit



ϵ_1

ϵ_2



ϵ^*

$$D = \epsilon E$$

$$\nabla \cdot D = 0$$

$$\nabla \times E = 0$$

$$\langle D \rangle = \epsilon^* \langle E \rangle$$

p_1, p_2 = volume fractions of
the components

$$\epsilon^* = \epsilon^* \left(\frac{\epsilon_1}{\epsilon_2}, \text{ composite geometry} \right)$$

**What are the effective propagation characteristics
of an EM wave (radar, microwaves) in the medium?**

Analytic Continuation Method for Homogenization

Bergman (1978), Milton (1979), Golden and Papanicolaou (1983), Theory of Composites, Milton (2002)

Stieltjes integral representation for homogenized parameter

separates geometry from parameters

$$F(s) = 1 - \frac{\epsilon^*}{\epsilon_2} = \int_0^1 \frac{d\mu(z)}{s - z}$$

← geometry

← material parameters

$$s = \frac{1}{1 - \epsilon_1 / \epsilon_2}$$

μ

- spectral measure of self adjoint operator $\Gamma\chi$
- mass = p_1
- higher moments depend on n -point correlations

$$\Gamma = \nabla(-\Delta)^{-1}\nabla.$$

χ = characteristic function of the brine phase

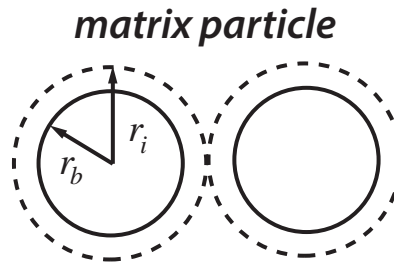
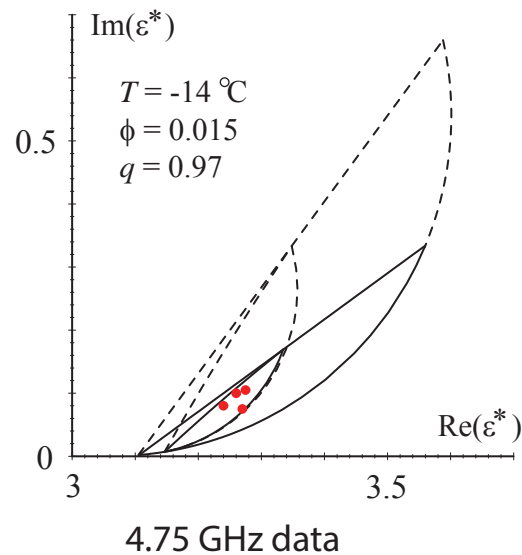
$$E = s (s + \Gamma\chi)^{-1} e_k$$

$\Gamma\chi$: microscale \rightarrow macroscale

$\Gamma\chi$ *links scales*

forward and inverse bounds on the complex permittivity of sea ice

forward bounds



$$q = r_b / r_i$$

$$0 < q < 1$$

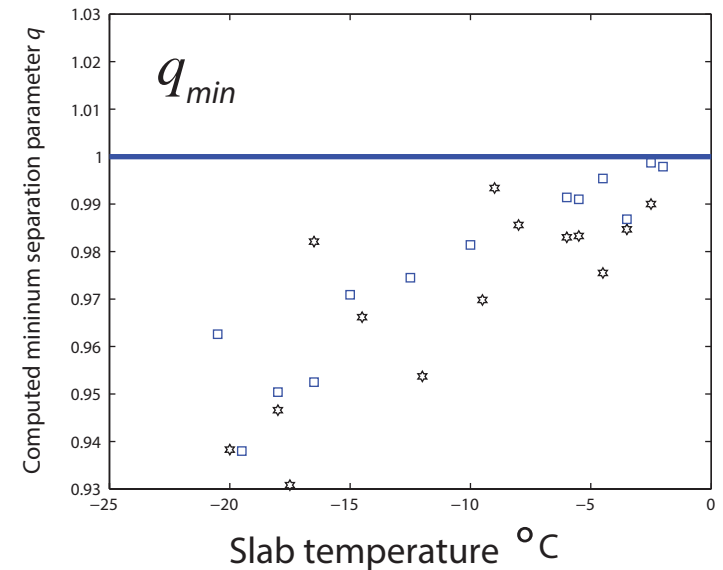
Golden 1995, 1997

Bruno 1991

inverse bounds and recovery of brine porosity

**Gully, Backstrom, Eicken, Golden
Physica B, 2007**

inverse bounds



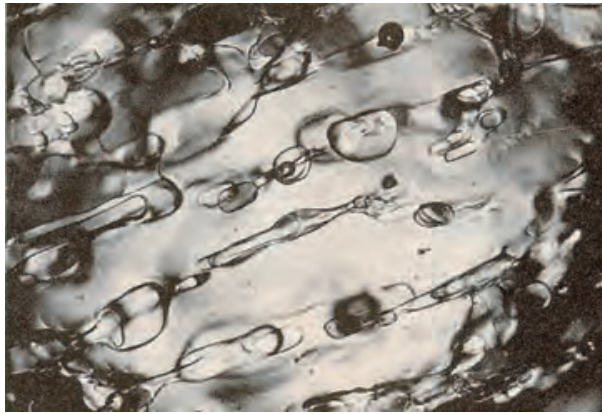
inversion for brine inclusion separations in sea ice from measurements of effective complex permittivity ϵ^*

rigorous inverse bound on spectral gap

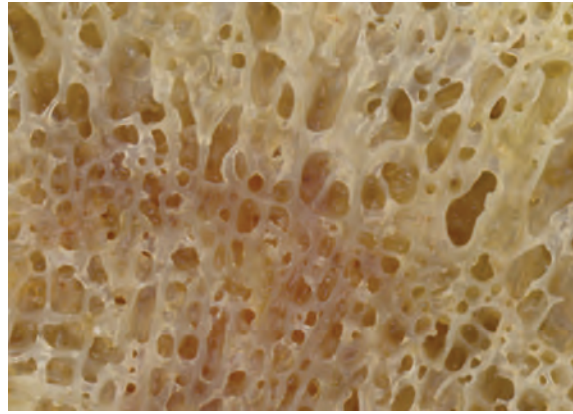
construct algebraic curves which bound admissible region in (p, q) -space

**Orum, Cherkaev, Golden
Proc. Roy. Soc. A, 2012**

SEA ICE

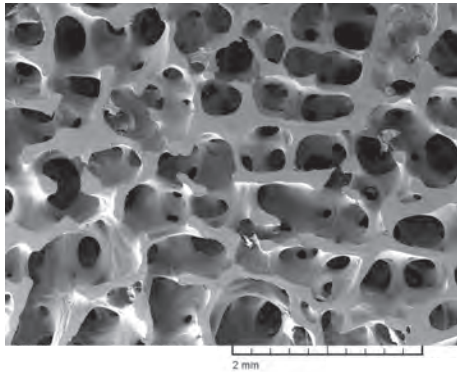


HUMAN BONE

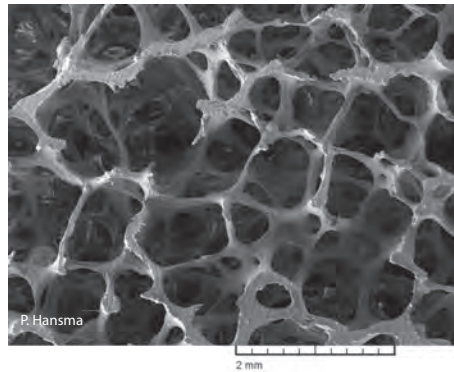


*spectral characterization
of porous microstructures
in human bone*

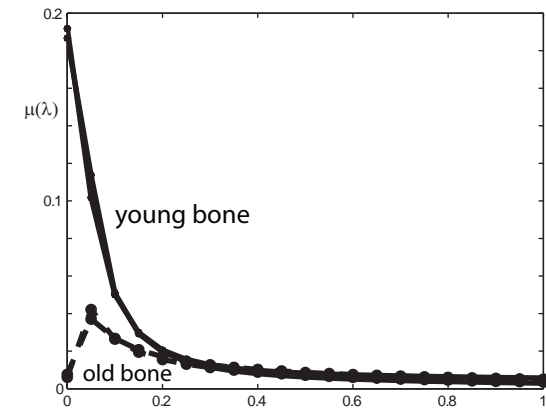
young healthy trabecular bone



old osteoporotic trabecular bone



reconstruct spectral measures
from complex permittivity data



use regularized inversion scheme

*apply spectral measure analysis of brine connectivity and
spectral inversion to electromagnetic monitoring of osteoporosis*

Golden, Murphy, Cherkaev, J. Biomechanics 2011

the math doesn't care if it's sea ice or bone!

direct calculation of spectral measures

Murphy, Hohenegger, Cherkaev, Golden, *Comm. Math. Sci.* 2015

- depends only on the composite geometry
- discretization of microstructural image gives binary network
- fundamental operator becomes a random matrix
- spectral measure computed from eigenvalues and eigenvectors

**once we have the spectral measure μ it can be used in
Stieltjes integrals for other transport coefficients:**

***electrical and thermal conductivity, complex permittivity,
magnetic permeability, diffusion, fluid flow properties***

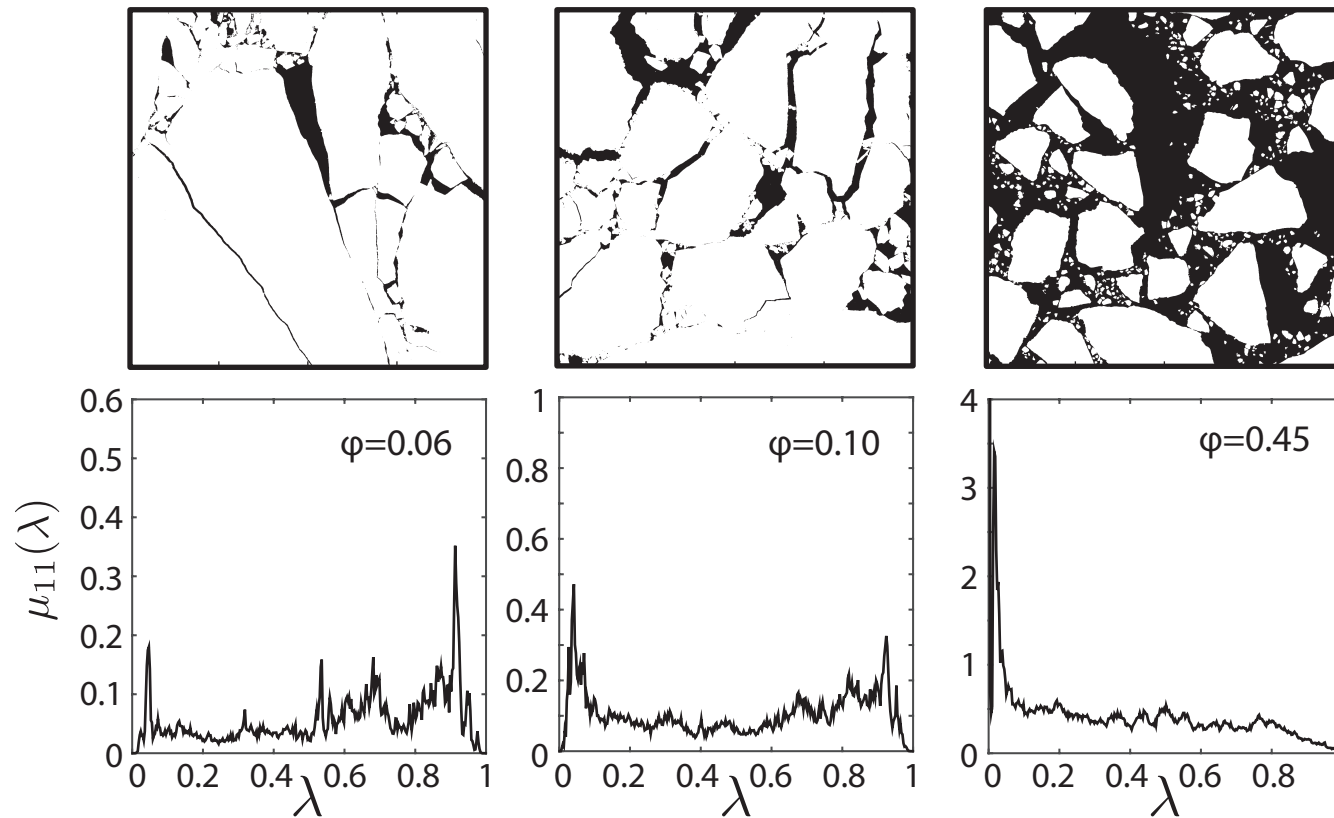
earlier studies of spectral measures

Day and Thorpe 1996

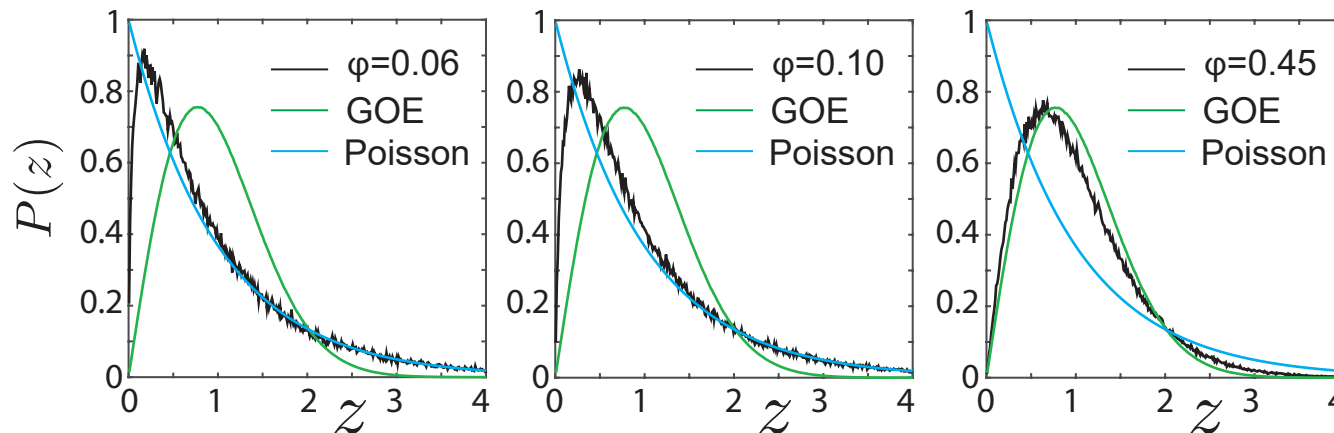
Helsing, McPhedran, Milton 2011

Spectral computations for sea ice floe configurations

spectral
measures



eigenvalue
spacing
distributions



uncorrelated

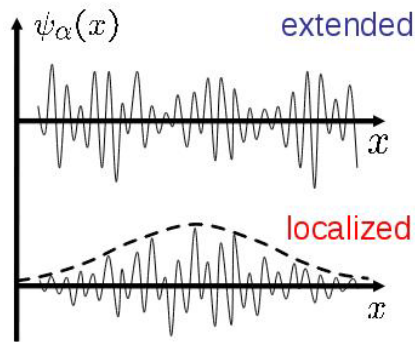


level repulsion

ANDERSON TRANSITION

**UNIVERSAL
Wigner-Dyson
distribution**

Murphy, Cherkhev, Golden
Phys. Rev. Lett. 2017



metal / insulator transition **localization**

Anderson 1958
Mott 1949
Shklovshii et al 1993
Evangelou 1992

**Anderson transition in wave physics:
quantum, optics, acoustics, water waves, ...**

we find a surprising analog

Anderson transition for classical transport in composites

Murphy, Cherkaev, Golden Phys. Rev. Lett. 2017

**PERCOLATION
TRANSITION**



**transition to universal
eigenvalue statistics (GOE)
extended states, mobility edges**

-- but without wave interference or scattering effects ! --

Eigenvalue Statistics of Random Matrix Theory

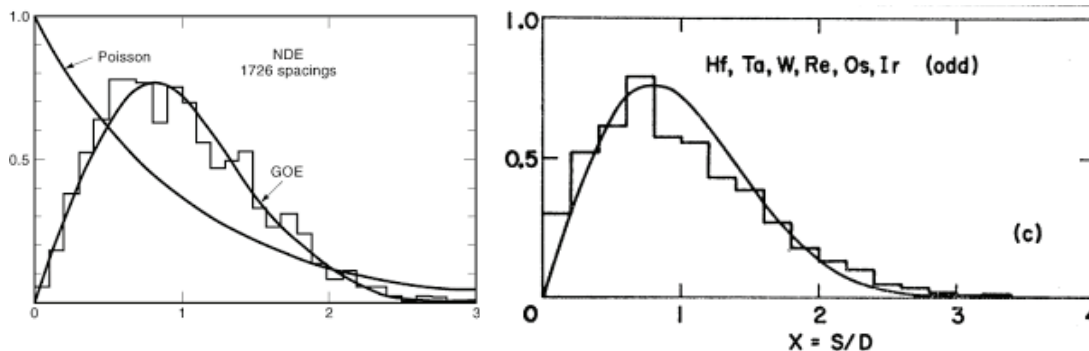
Wigner (1951) and Dyson (1953) first used random matrix theory (RMT) to describe quantized energy levels of heavy atomic nuclei.

$[N]_{ij} \sim N(0,1), \quad A = (N + N^T)/2 \quad \text{Gaussian orthogonal ensemble (GOE)}$

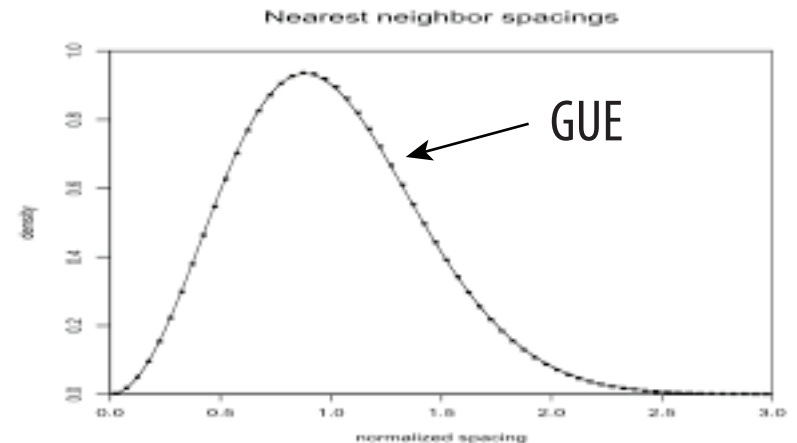
$[N]_{ij} \sim N(0,1) + iN(0,1), \quad A = (N + N^\dagger)/2 \quad \text{Gaussian unitary ensemble (GUE)}$

Short range and long range correlations of eigenvalues are measured by various eigenvalue statistics.

Spacing distributions of energy levels for heavy atomic nuclei



Spacing distributions of the first billion zeros of the Riemann zeta function



RMT used to characterize **disorder-driven transitions** in mesoscopic conductors, neural networks, random graph theory, etc.

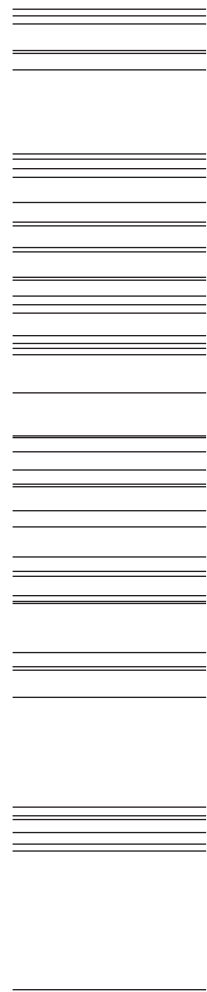
Universal eigenvalue statistics arise in a broad range of “unrelated” problems!

Transition in Eigenvalue Correlations

$$P(z) = \exp(-z)$$

Eigenvalue Spacing Distribution

**Poisson
Spectra**

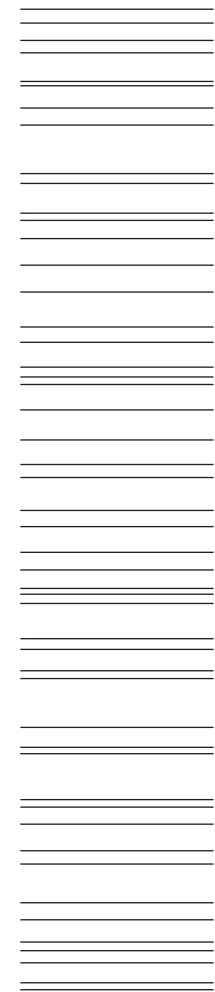


Uncorrelated

$$P(z) \approx \frac{\pi z}{2} \exp(-\pi z^2/4) \quad \text{Wigner surmise}$$

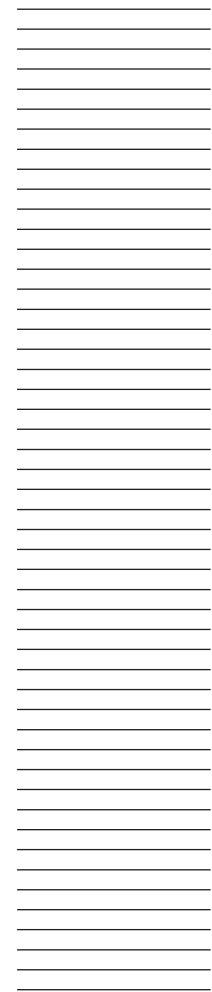
Eigenvalue Spacing Distribution

**GOE
Spectra**



**Highly
Correlated**

**Picket
Fence**



**Completely
Correlated**

**Connectedness
Phase Transition**



**LEVEL
REPULSION**



eigenvector localization and mobility edges

Inverse Participation Ratio:
$$I(\vec{v}_n) = \sum_{i=1}^N |(\vec{v}_n)_i|^4$$

Completely Localized:
$$I(\vec{e}_n) = 1$$

Completely Extended:
$$I\left(\frac{1}{\sqrt{N}} \vec{1}\right) = \frac{1}{N}$$

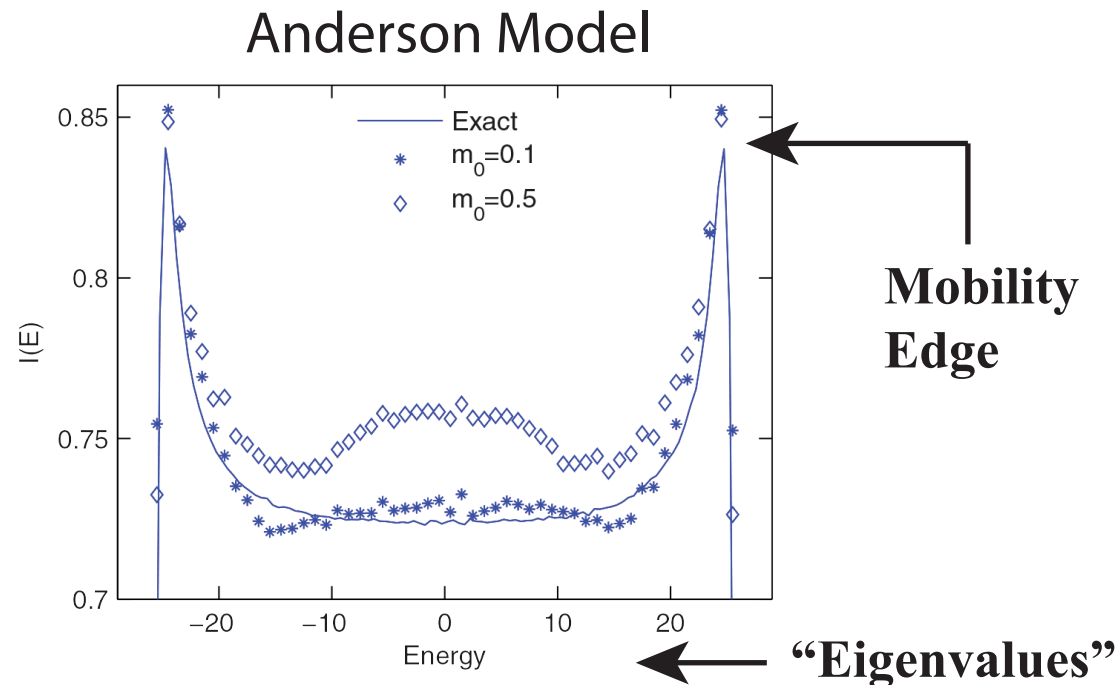
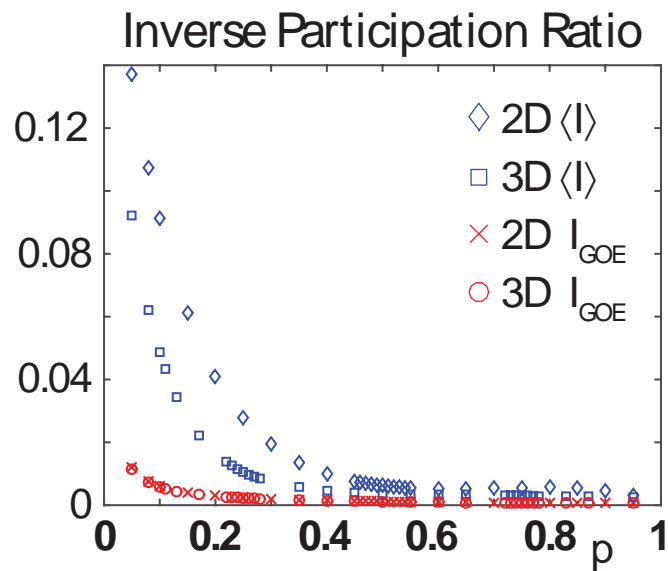
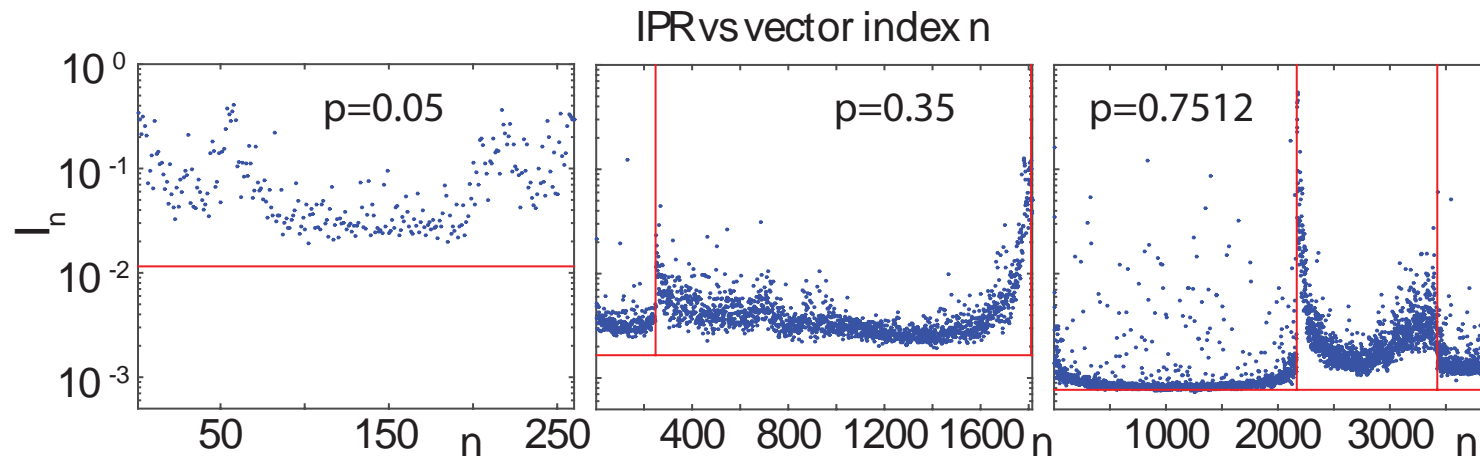


FIG. 4. (Color online) IPR for Anderson model in two dimensions with $x = 6.25$ ($w = 50$) from exact diagonalization (solid line) and from LDRG with different values of the cutoff m_0 . LDRG data are averaged over 100 runs of systems with 100×100 sites.

Localization properties of eigenvectors in random resistor networks

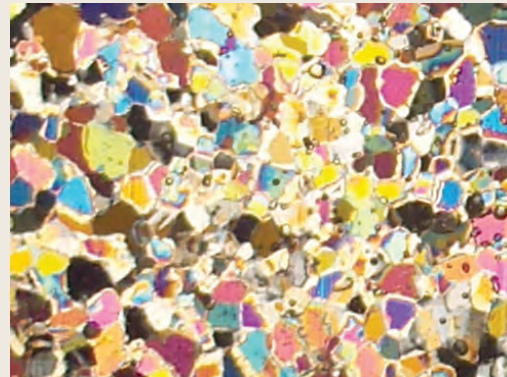


$$I_n = \sum_i (\vec{v}_n)_i^4$$

Bounds on the complex permittivity of polycrystalline materials by analytic continuation

Adam Gully, Joyce Lin,
Elena Cherkaev, Ken Golden

- **Stieltjes integral representation for effective complex permittivity**
Milton (1981, 2002), Barabash and Stroud (1999), ...
- **Forward and inverse bounds**
orientation statistics
- **Applied to sea ice using two-scale homogenization**
- **Inverse bounds give method for distinguishing ice types using remote sensing techniques**



PROCEEDINGS A

350 YEARS
OF SCIENTIFIC
PUBLISHING

An invited review
commemorating 350 years
of scientific publishing at the
Royal Society

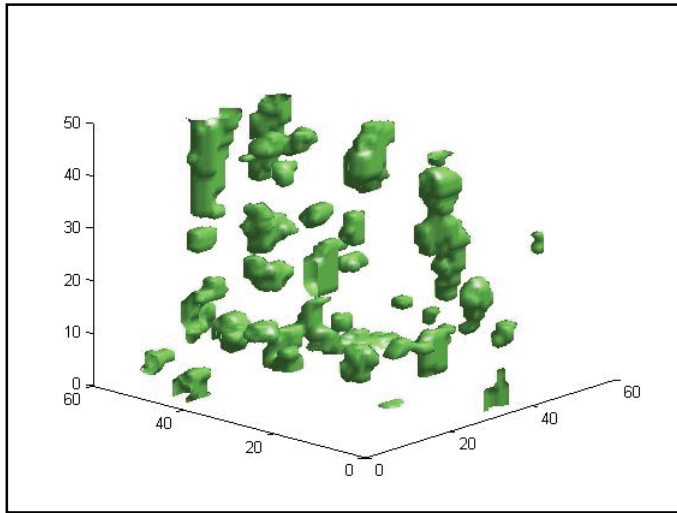
A method to distinguish
between different types
of sea ice using remote
sensing techniques

A computer model to
determine how a human
should walk so as to expend
the least energy

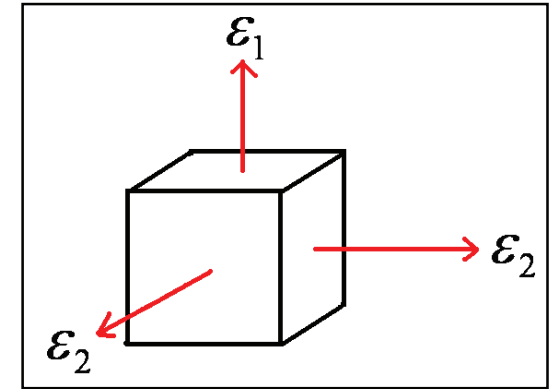


THE
ROYAL
SOCIETY
PUBLISHING

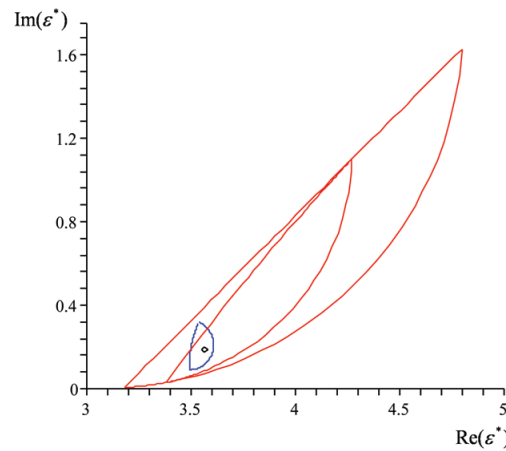
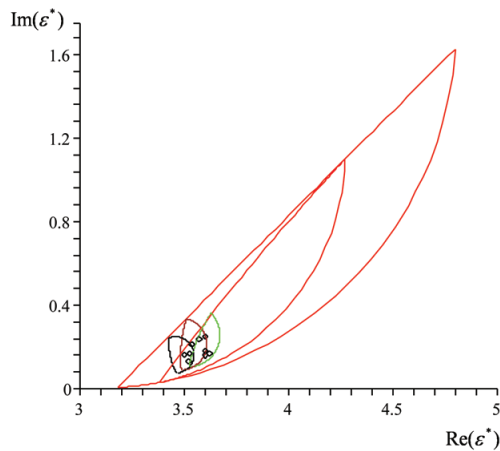
two scale homogenization for polycrystalline sea ice



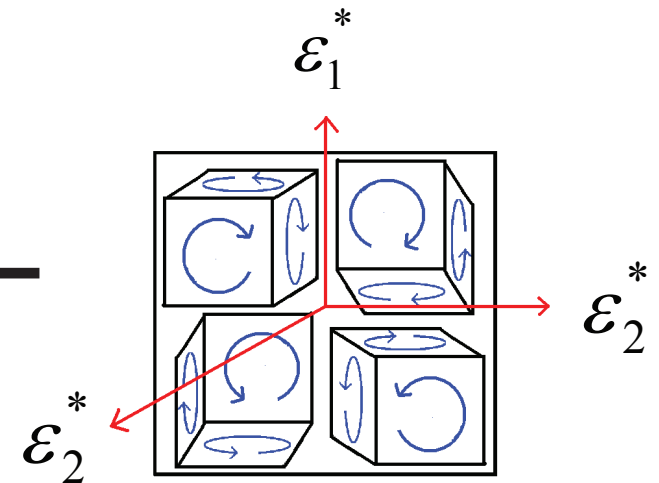
numerical homogenization
for single crystal



analytic continuation
for polycrystals



bounds

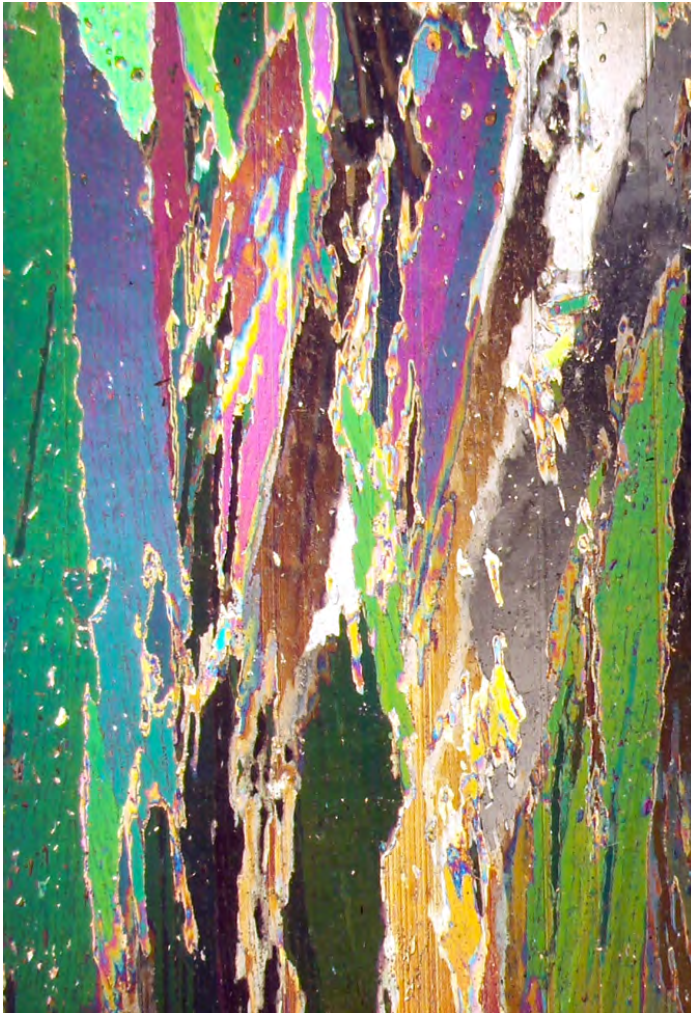


higher threshold for fluid flow in Antarctic granular sea ice

columnar

granular

5%



10%



Golden, Sampson, Gully, Lubbers, Tison 2019

Rigorous bounds on the complex permittivity tensor of sea ice with polycrystalline anisotropy within the horizontal plane

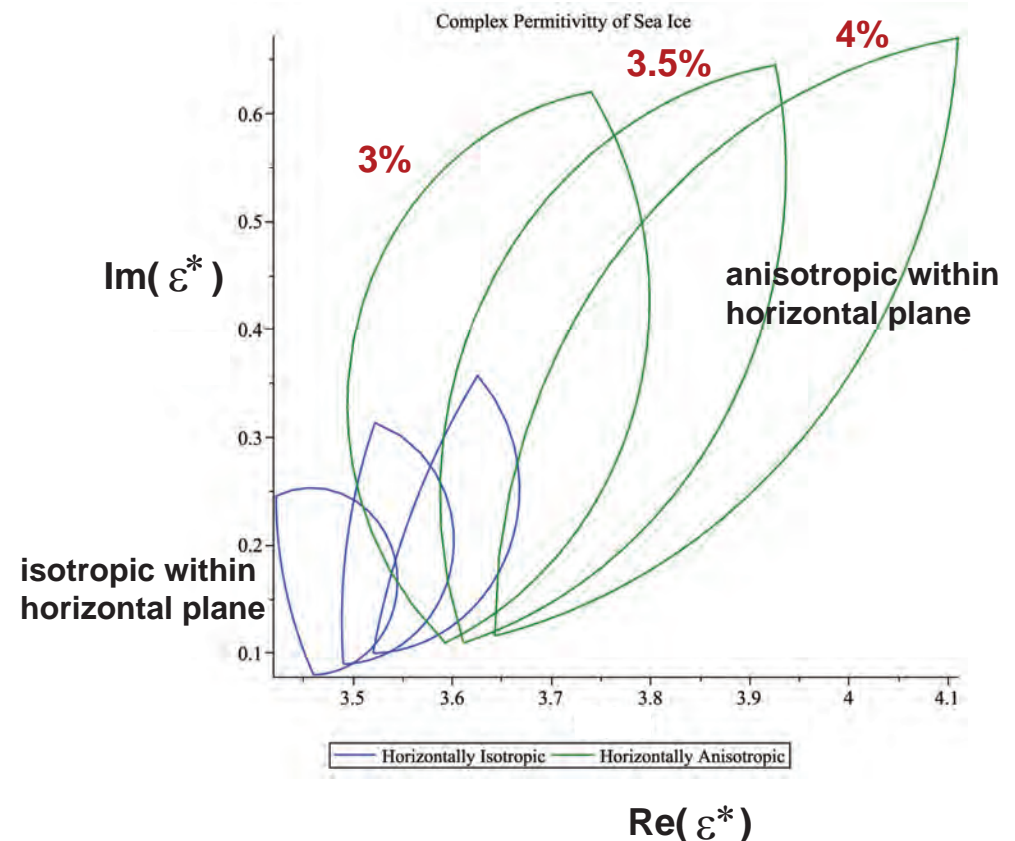
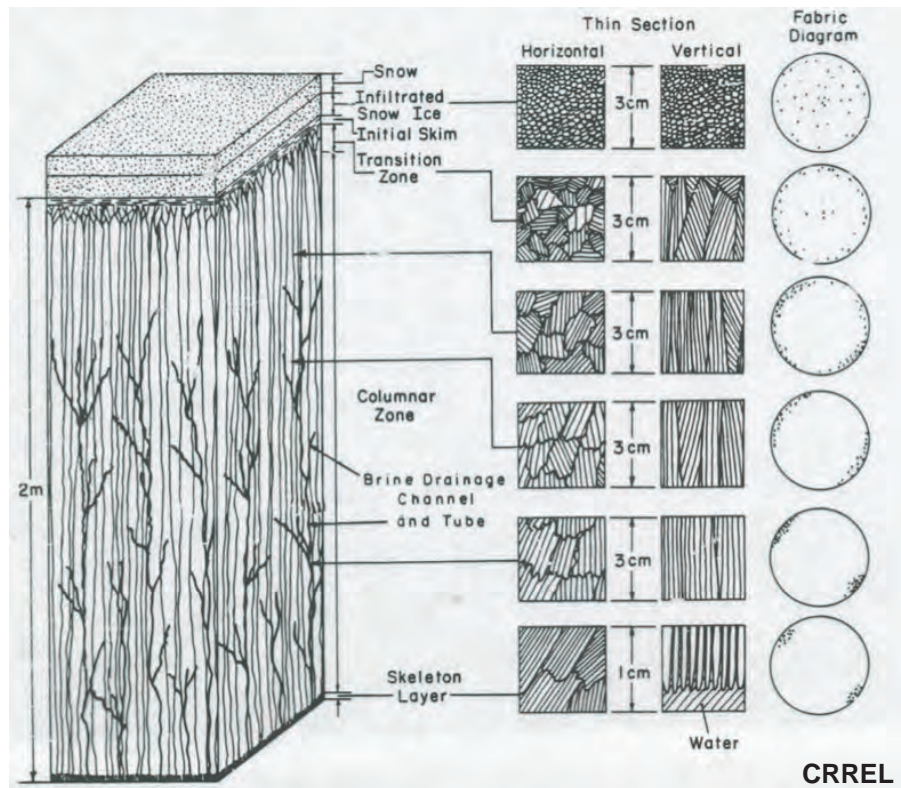
McKenzie McLean, Elena Cherkaev, Ken Golden 2019

motivated by Weeks and Gow, *JGR* 1979: c-axis alignment in Arctic fast ice off Barrow

Golden and Ackley, *JGR* 1981: radar propagation model in aligned sea ice

input: orientation statistics

output: bounds



advection enhanced diffusion

effective diffusivity

nutrient and salt transport in sea ice
heat transport in sea ice with convection
sea ice floes in winds and ocean currents
tracers, buoys diffusing in ocean eddies
diffusion of pollutants in atmosphere

advection diffusion equation with a velocity field \vec{u}

$$\frac{\partial T}{\partial t} + \vec{u} \cdot \vec{\nabla} T = \kappa_0 \Delta T$$

$$\vec{\nabla} \cdot \vec{u} = 0$$



homogenize

$$\frac{\partial \bar{T}}{\partial t} = \kappa^* \Delta \bar{T}$$

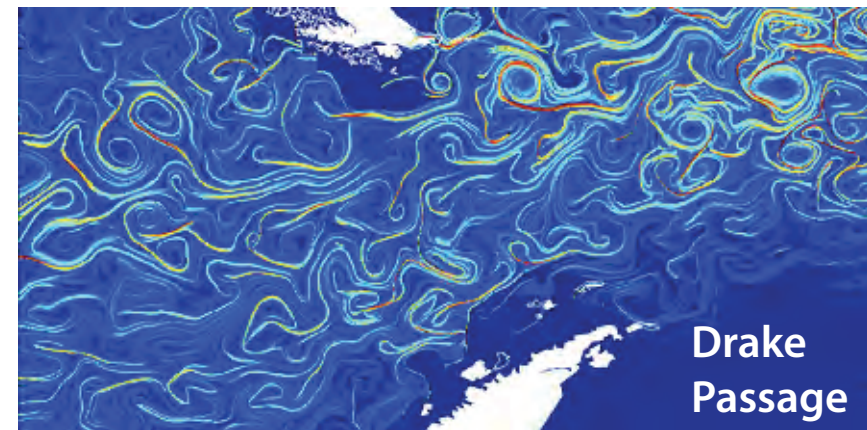
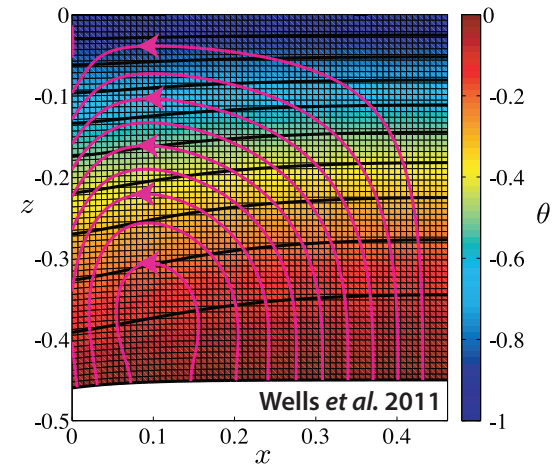
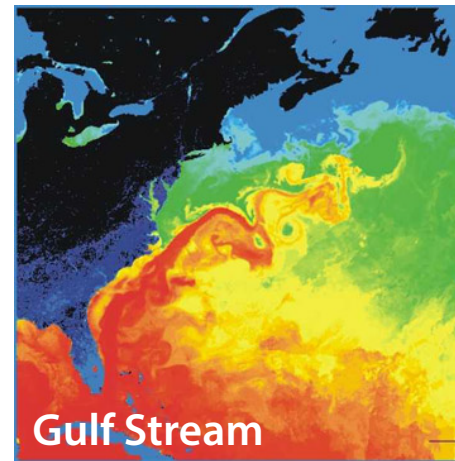
κ^* effective diffusivity

Stieltjes integral for κ^* with spectral measure

Avellaneda and Majda, PRL 89, CMP 91

Murphy, Cherkaev, Xin, Zhu, Golden, *Ann. Math. Sci. Appl.* 2017

Murphy, Cherkaev, Zhu, Xin, Golden, *J. Math. Phys.* 2019



Stieltjes Integral Representation for Advection Diffusion

Murphy, Cherkaev, Zhu, Xin, Golden, *J. Math. Phys.* 2019

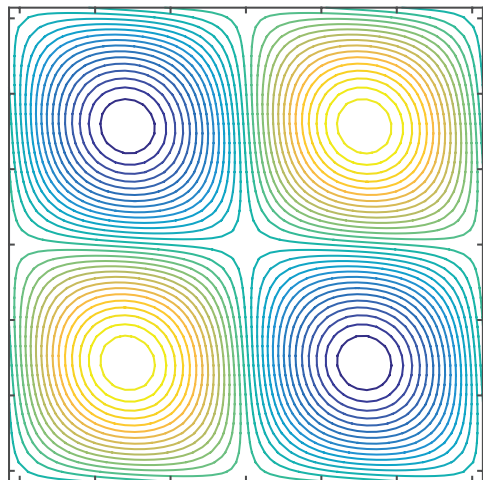
$$\kappa^* = \kappa \left(1 + \int_{-\infty}^{\infty} \frac{d\mu(\tau)}{\kappa^2 + \tau^2} \right), \quad F(\kappa) = \int_{-\infty}^{\infty} \frac{d\mu(\tau)}{\kappa^2 + \tau^2}$$

- μ is a positive definite measure corresponding to the spectral resolution of the self-adjoint operator $i\Gamma H\Gamma$
- H = stream matrix , κ = local diffusivity
- $\Gamma := -\nabla(-\Delta)^{-1}\nabla$, Δ is the Laplace operator
- $i\Gamma H\Gamma$ is bounded for time independent flows
- $F(\kappa)$ is analytic off the spectral interval in the κ -plane

separation of material properties and flow field
spectral measure calculations

Rigorous bounds on convection enhanced thermal conductivity of sea ice

Kraitzman, Hardenbrook, Murphy, Zhu, Cherkaev, Strong, Golden 2019

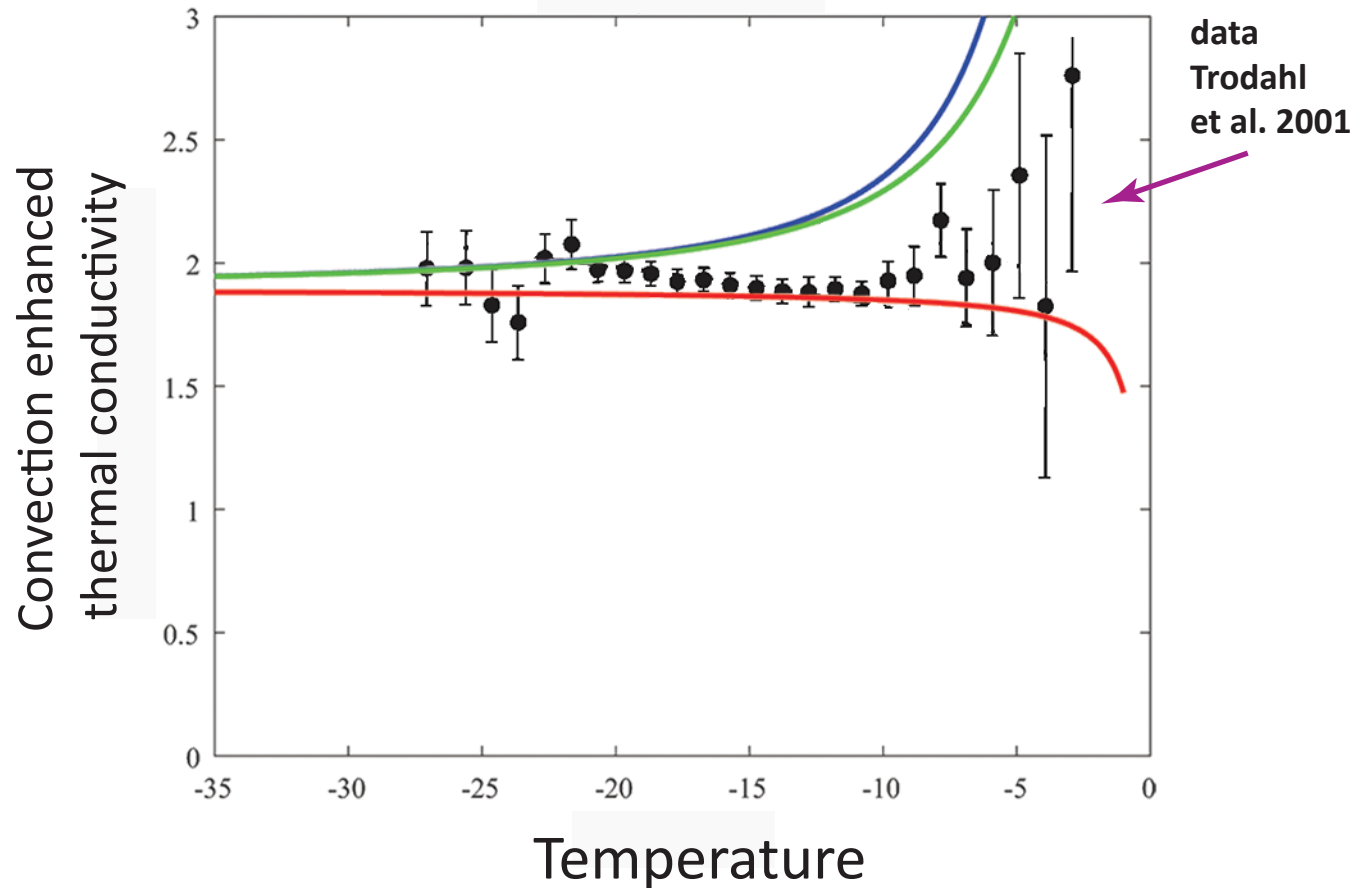


cat's eye flow model for
brine convection cells

similar bounds
for shear flows

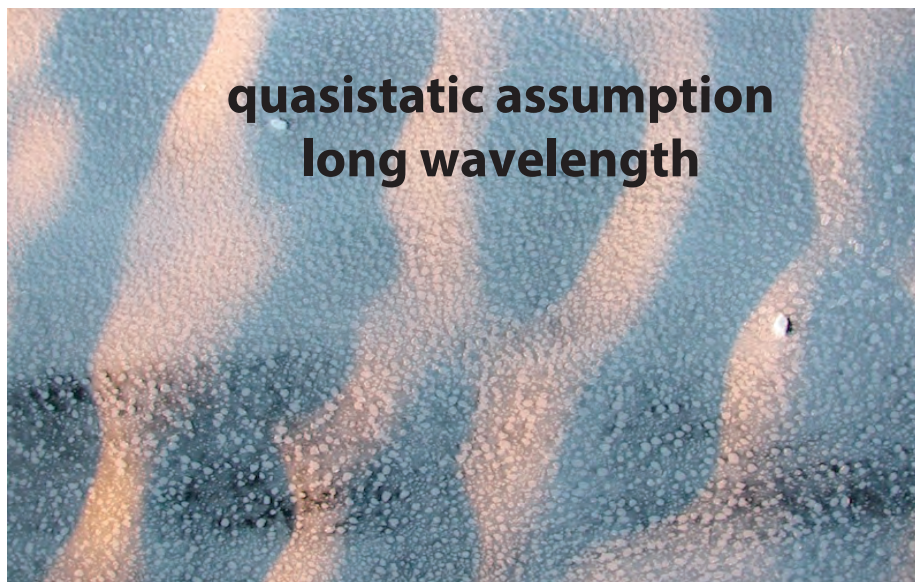
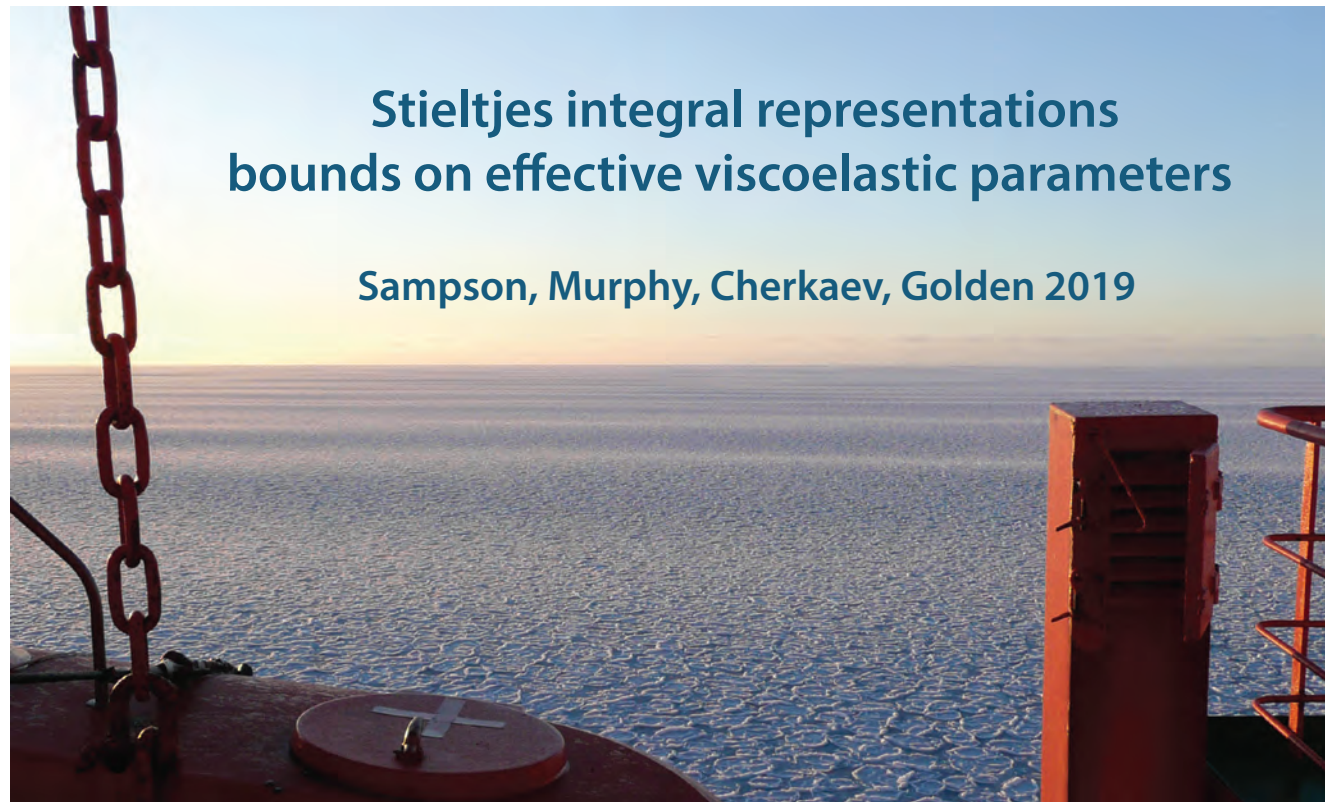
**rigorous bounds assuming information
on flow field INSIDE inclusions**

Kraitzman, Cherkaev, Golden
SIAM J. Appl. Math (in revision), 2019

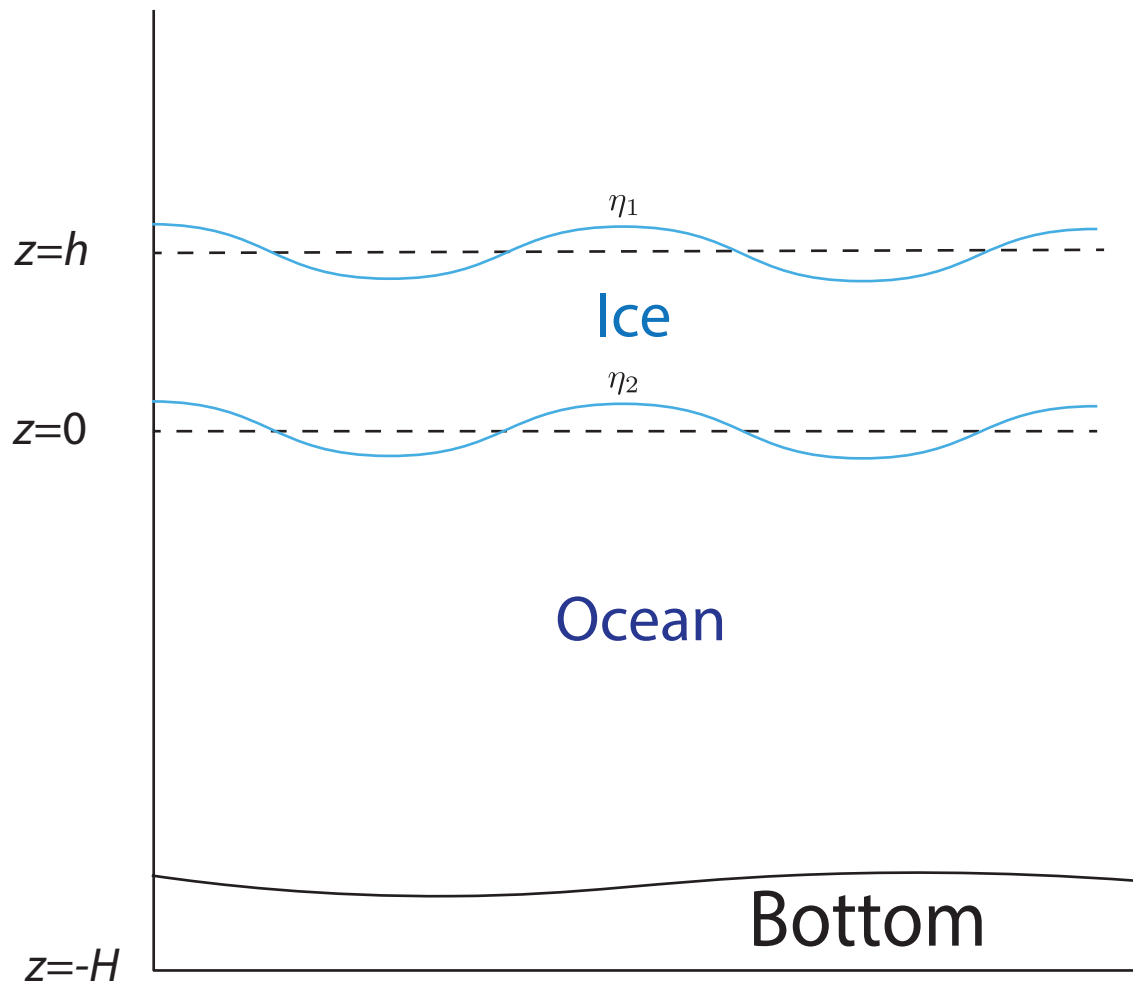


rigorous Padé bounds from Stieltjes integral +
analytical calculations of moments of measure

wave propagation in the marginal ice zone



Two Layer Models and Effective Rheological Parameters



Viscous fluid layer (Keller 1998)

Effective Viscosity ν

Equations of motion:
$$\frac{\partial U}{\partial t} = -\frac{1}{\rho} \nabla P + \nu \nabla^2 U + g$$

Viscoelastic fluid layer (Wang-Shen 2010)

Effective Complex Viscosity $\nu_e = \nu + iG/\rho\omega$

Equations of motion
$$\frac{\partial U}{\partial t} = -\frac{1}{\rho} \nabla P + \nu_e \nabla^2 U + g$$

Viscoelastic thin beam (Mosig *et al.* 2015)

Effective Complex Shear Modulus $G_v = G - i\omega\rho\nu$

Stieltjes integral representation for effective complex viscoelastic parameter; bounds

Sampson, Murphy, Cherkaev, Golden 2019

G shear modulus
 ν viscosity
 P pressure
 λ Poisson ratio
 ω angular frequency
 ρ density
 U velocity field
 g gravity

Homogenization for two phase viscoelastic composite

microscale

$$\sigma = C_{ijkl} \epsilon_{kl} = C : \epsilon$$

macroscale

$$\langle \sigma \rangle = C^* : \langle \epsilon \rangle$$

$$\langle \epsilon \rangle = \epsilon^0$$

quasistatic assumption

$$\nabla \cdot \sigma = 0$$

Resolvent

$$\epsilon = \left(1 - \frac{1}{s} \Gamma \chi_1\right)^{-1} \epsilon^0 \quad \rightarrow \quad \frac{v^*}{v_2} = \left(1 - \|\epsilon^0\|^{-2} F(s)\right)$$

$$\Gamma = \nabla^s (\nabla \cdot \nabla^s)^{-1} \nabla \cdot$$

$$V_1 = 10^7 + i 4875 \quad \text{pancake ice}$$

$$V_2 = 5 + i 0.0975 \quad \text{slush / frazil}$$

$$C = 2(\chi_1 v_1 + \chi_2 v_2) \Lambda_s$$



Strain Field

$$\epsilon = \frac{1}{2} [\nabla u + (\nabla u)^T] = \nabla^s u \quad \nabla \cdot u = 0$$

$$F(s) = \int_0^1 \frac{d\mu(\lambda)}{s - \lambda} \quad s = \frac{1}{1 - \frac{v_1}{v_2}}$$

bounds on the effective complex viscoelasticity

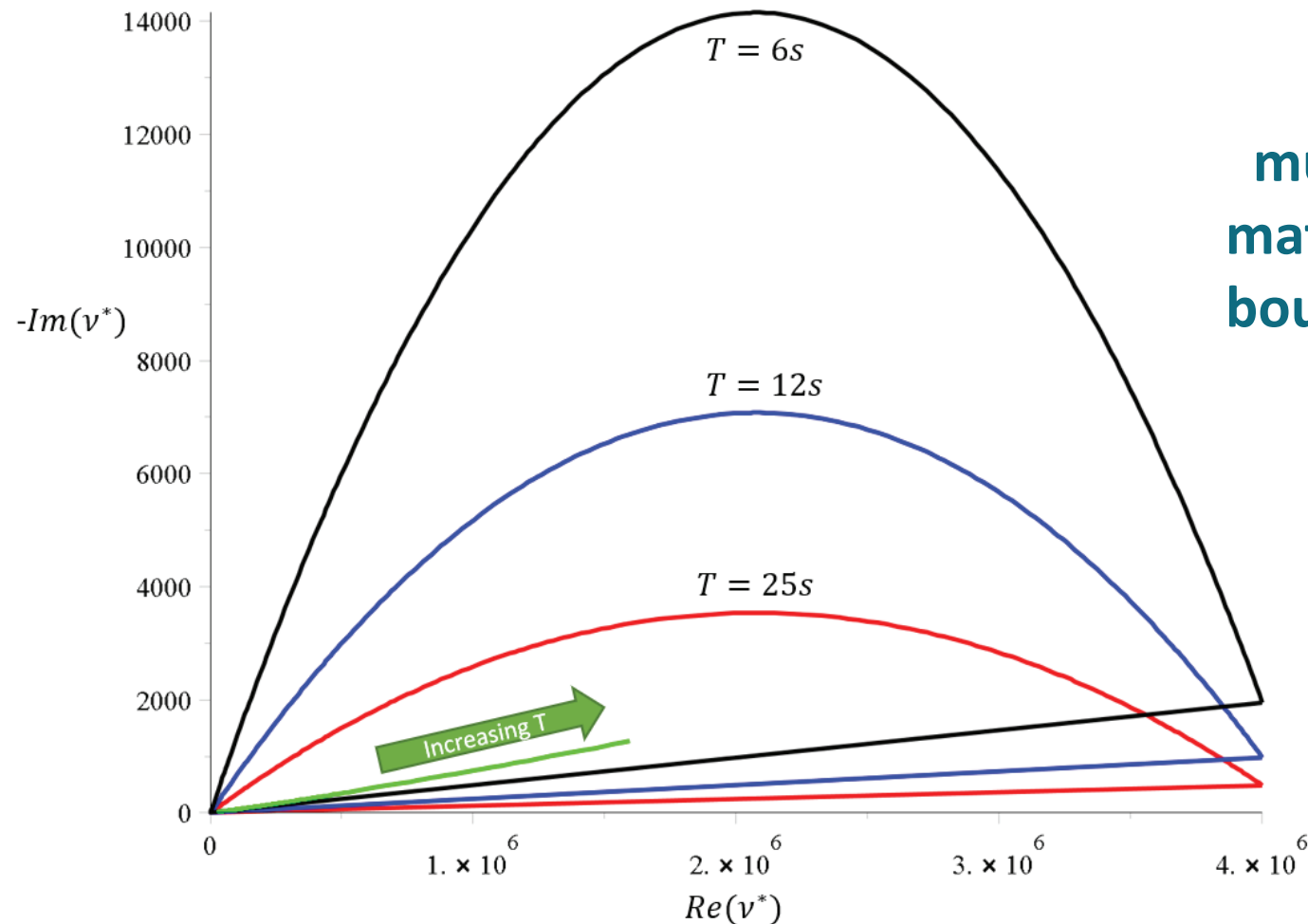
complex elementary bounds
(fixed area fraction of floes)

$$V_1 = 10^7 + i 4875$$

pancake ice

$$V_2 = 5 + i 0.0975$$

slush / frazil



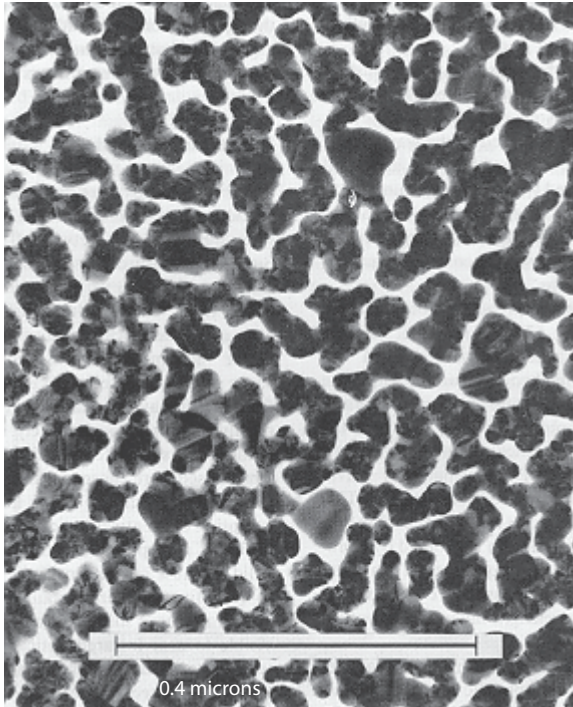
+
much tighter
matrix particle
bounds + data

Sampson, Murphy, Cherkaev, Golden 2019

Interaction of light with sea ice

thin silver film

microns



(Davis, McKenzie, McPhedran, 1991)

Arctic melt ponds

kilometers



(Perovich, 2005)



optical properties

composite geometry -- area fraction of phases, connectedness, necks

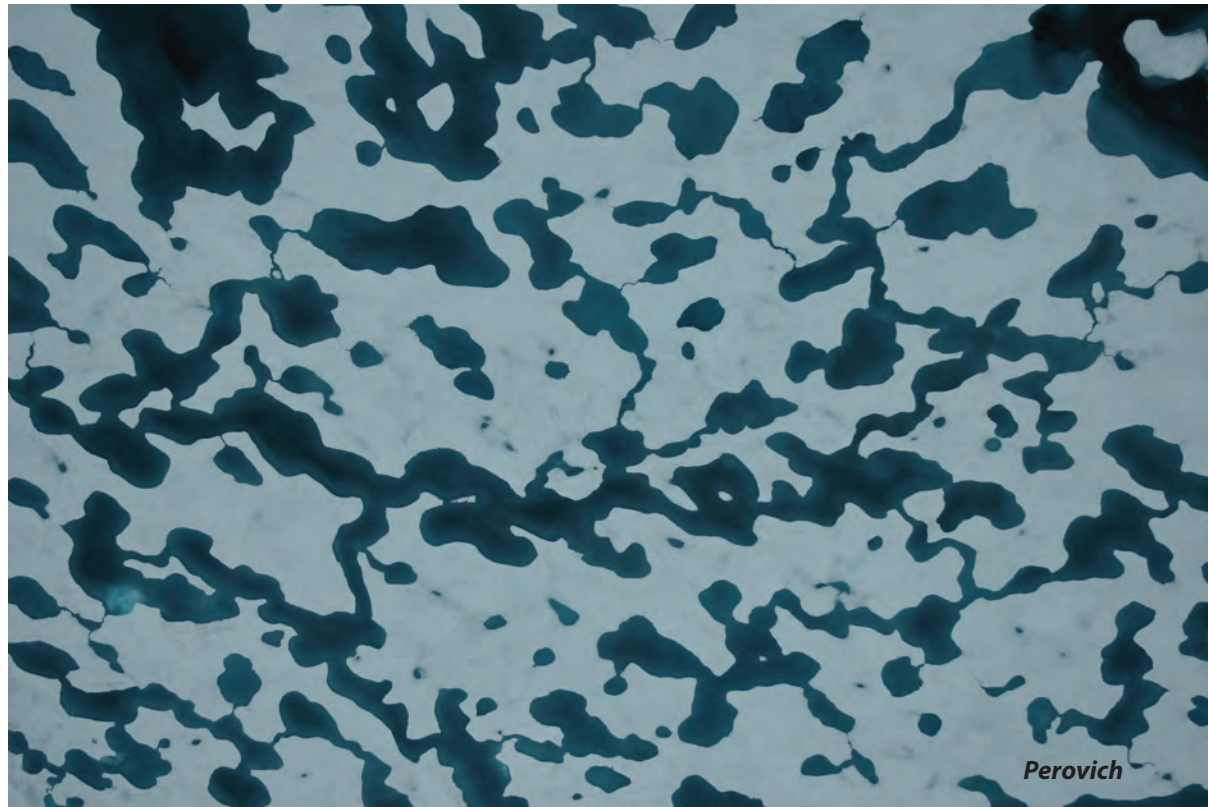
melt pond formation and albedo evolution:

- *major drivers in polar climate*
- *key challenge for global climate models*

numerical models of melt pond evolution, including topography, drainage (permeability), etc.

Lüthje, Feltham,
Taylor, Worster 2006
Flocco, Feltham 2007

Skyllingstad, Paulson,
Perovich 2009
Flocco, Feltham,
Hunke 2012



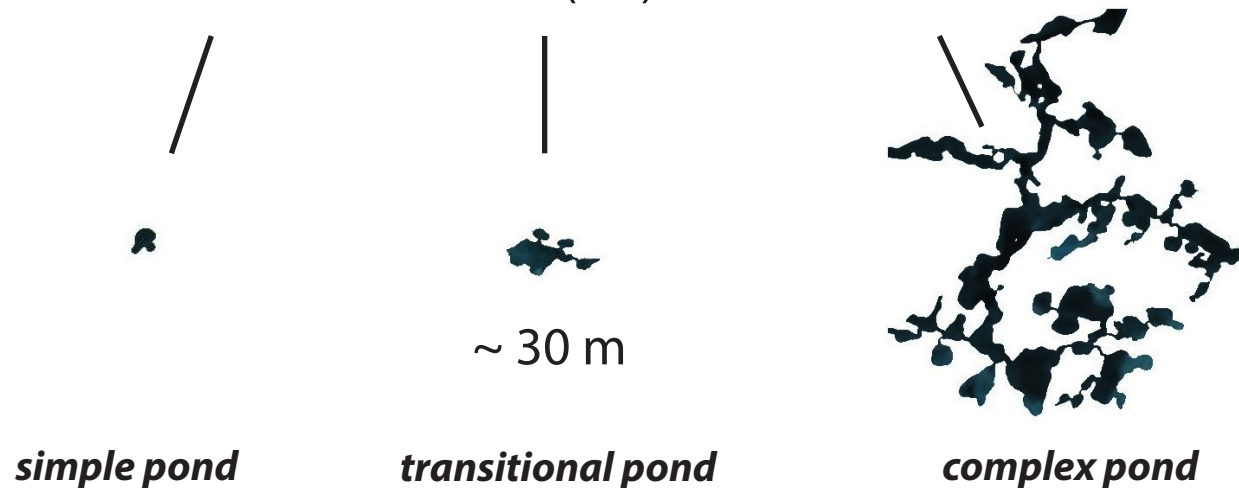
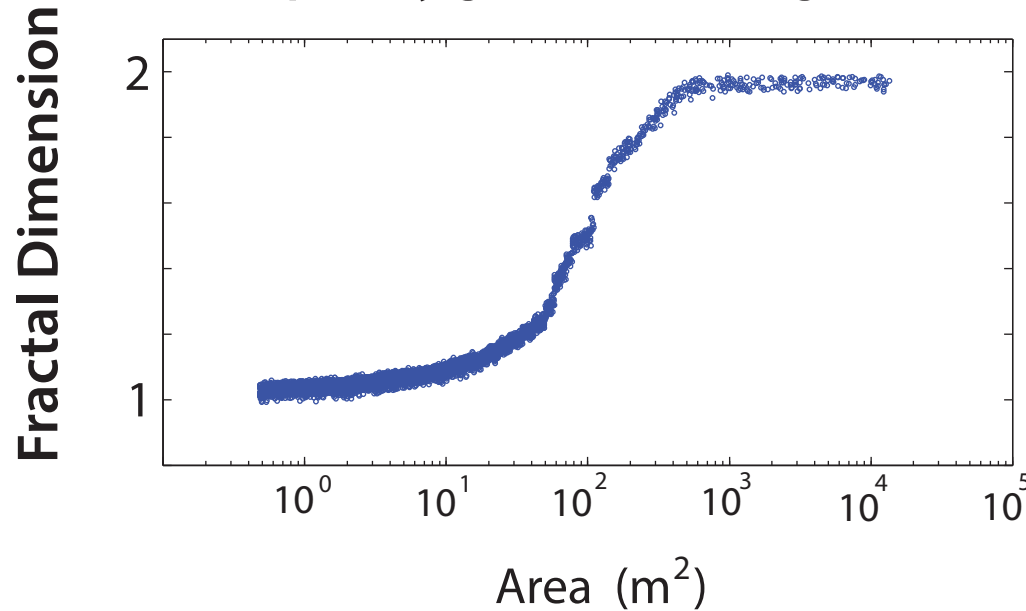
Are there universal features of the evolution similar to phase transitions in statistical physics?

Transition in the fractal geometry of Arctic melt ponds

Christel Hohenegger, Bacim Alali, Kyle Steffen, Don Perovich, Ken Golden

The Cryosphere, 2012

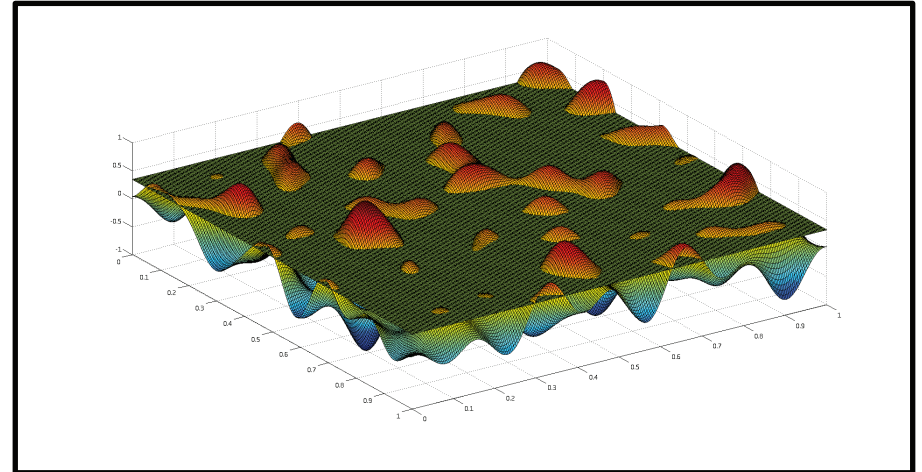
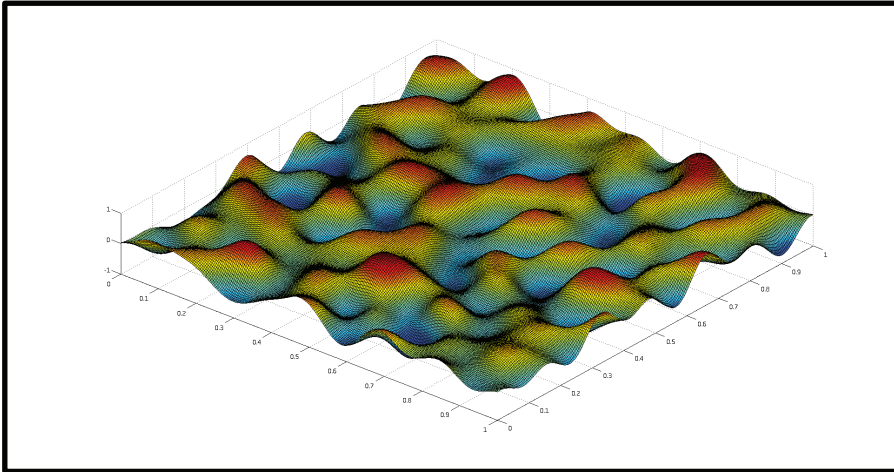
complexity grows with length scale



Continuum percolation model for melt pond evolution

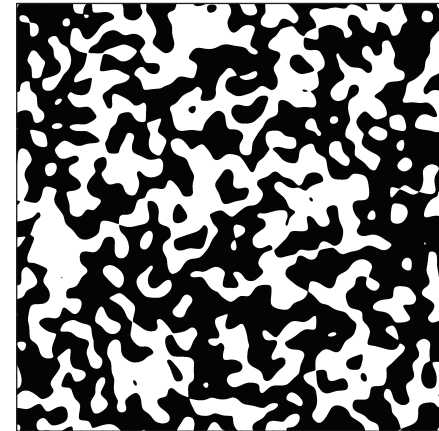
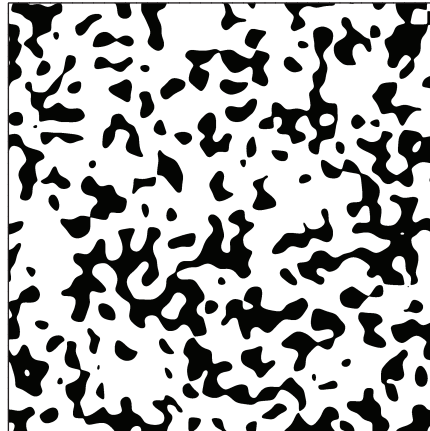
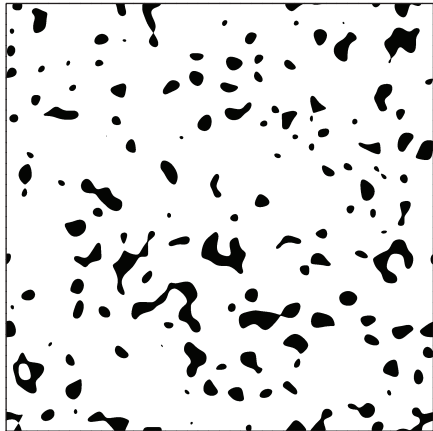
level sets of random surfaces

Brady Bowen, Court Strong, Ken Golden, J. Fractal Geometry 2018



random Fourier series representation of surface topography

intersections of a plane with the surface define melt ponds

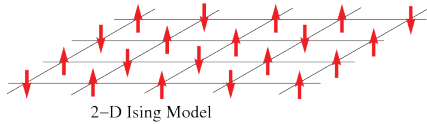


electronic transport in disordered media

diffusion in turbulent plasmas

Isichenko, Rev. Mod. Phys., 1992

Ising model for ferromagnets \longrightarrow Ising model for melt ponds



Ma, Sudakov, Strong, Golden, *New J. Phys.* 2019

$$\mathcal{H}_\omega = -J \sum_{\langle i,j \rangle} s_i s_j - \sum_i H_i s_i$$

$$s_i = \begin{cases} \uparrow & +1 \\ \downarrow & -1 \end{cases}$$

water (spin up)

ice (spin down)

random magnetic field
represents snow topography

magnetization $M = \lim_{N \rightarrow \infty} \frac{1}{N} \left\langle \sum_j s_j \right\rangle$

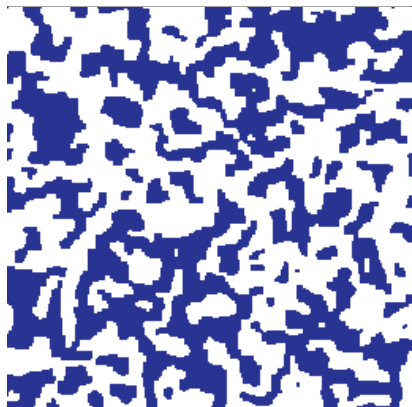
pond coverage $\sim \text{albedo}$ $\frac{(M+1)}{2}$

only nearest neighbor
patches interact

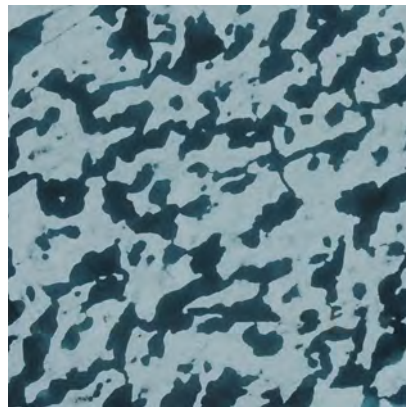
Starting with random initial configurations, as Hamiltonian energy is minimized by Glauber spin flip dynamics, system “flows” toward metastable equilibria.

Melt ponds are metastable islands of like spins.

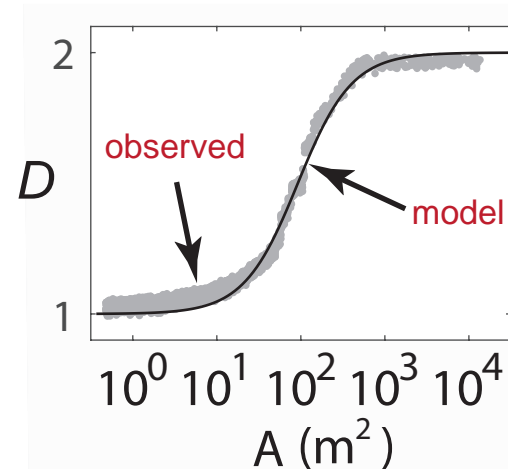
Order from Disorder



Ising
model



melt pond
photo (Perovich)



pond size distribution
exponent

observed -1.5

(Perovich, *et al.* 2002)

model -1.58

ONLY MEASURED INPUT = LENGTH SCALE (GRID SIZE) from snow topography data



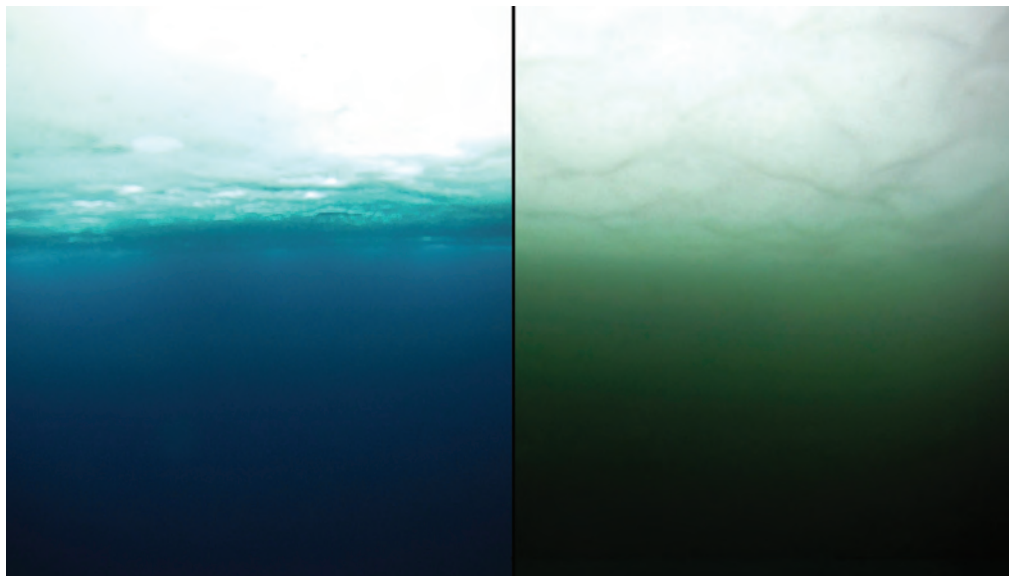
2011 massive under-ice **algal bloom**

Arrigo et al., *Science* 2012

melt ponds act as

WINDOWS

allowing light
through sea ice



no bloom

bloom

Have we crossed into a new ecological regime?

The frequency and extent of sub-ice
phytoplankton blooms in the Arctic Ocean

Horvat, Rees Jones, Iams, Schroeder,
Flocco, Feltham, *Science Advances*, 2017

The distribution of solar energy under
ponded sea ice

Horvat, Flocco, Rees Jones, Roach, Golden, 2019

(2015 AMS MRC)

The distribution of solar energy under ponded first-year sea ice

Horvat, Flocco, Rees Jones, Roach, Golden, *in revision*, 2019

- Model for 3D light field under ponded sea ice.
- Distribution of solar energy at depth influenced by *shape and connectivity* of melt ponds, as well as area fraction.
- Aggregate properties of the sub-ice light field, such as a significant enhancement of available solar energy under the ice, are controlled by parameter closely related to pond fractal geometry.
- Model and analysis explain how melt pond geometry *homogenizes* under-ice light field, affecting habitability.

Pond geometry affects the ecology of the Arctic Ocean.

Conclusions

1. Wave phenomena arise naturally in the sea ice system.
2. **Homogenization and statistical physics help *link scales*** and provide rigorous methods for finding effective behavior, and advance how sea ice is represented in climate models.
3. **Herglotz functions and Stieltjes integrals** provide powerful methods of homogenization for wave phenomena in sea ice structures.
4. Our research will help to **improve projections of climate change** and the fate of the Earth sea ice packs.

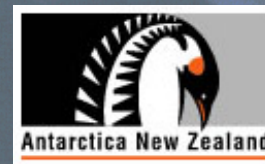
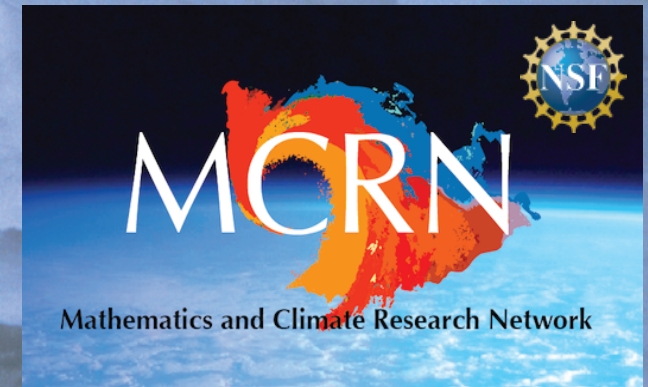
THANK YOU

Office of Naval Research

Applied and Computational Analysis Program
Arctic and Global Prediction Program

National Science Foundation

Division of Mathematical Sciences
Division of Polar Programs



Buchanan Bay, Antarctica Mertz Glacier Polynya Experiment July 1999

fluid permeability of a porous medium



how much water gets through the sample per unit time?

Darcy's Law

for slow viscous flow in a porous medium

averaged fluid velocity

pressure gradient

$$\mathbf{v} = -\frac{\mathbf{k}}{\eta} \nabla p$$

viscosity

\mathbf{k} = fluid permeability tensor

HOMOGENIZATION

mathematics for analyzing effective behavior of heterogeneous systems